Figure 10

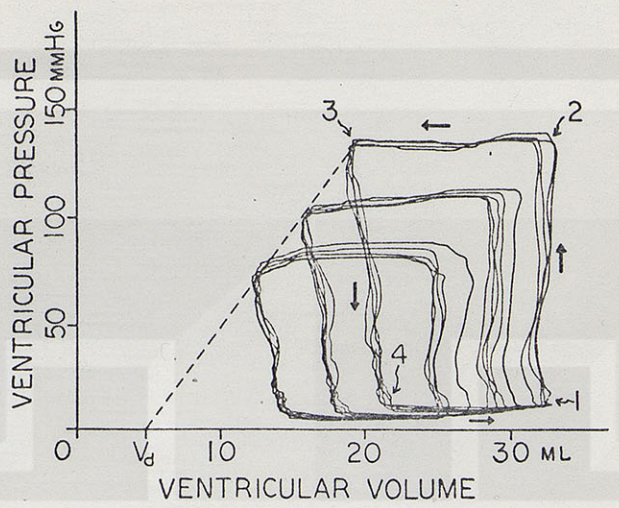

Graphical explanation of correction volume v_d. v_d is the volume axis intercept of the broken straight line which is drawn to connect the left uppermost corners of a family of pressure-volume loops traced under a control contractile state and different ventricular loading conditions above and below normal preload and afterload. v_d was 4 ~ 6 ml for 20-kg dogs and remained constant even when the contractile state was altered by epinephrine infusion. The arrows show the direction of movement of a pressure-volume data point on the pressure-volume loop. Isovolumetric contraction phase (1-2), systolic ejection phase (2-3), isovolumetric relaxation phase (3-4) and diastolic filling phase (4-1). (From: Suga, H. and Sagawa, K., Ann. Biomed. Eng. 1: 160, 1972.)

From our analysis thus far we would expect C_s to be primarily associated wtih"contractility". As $C_s \rightarrow$small, contractility would increase. For constant contractile state we would expect C_s to be consant. Experiments by Suga and Sagawa have confirmed this in dogs. They defined

$$e(t) = \frac{1}{C(t)} = \frac{P(t)}{(Q(t) - Q_o)},$$ and calculated it under a variety of experimental conditions. Note from Figure 11 that the peak valve of e(t) (corresponding to minimum C(t) or C_s) is unaffected by changes in arterial pressure, stroke volume, or heart rate but is dramatically increased by the inotropic hormone epinephrine.

Figure 11

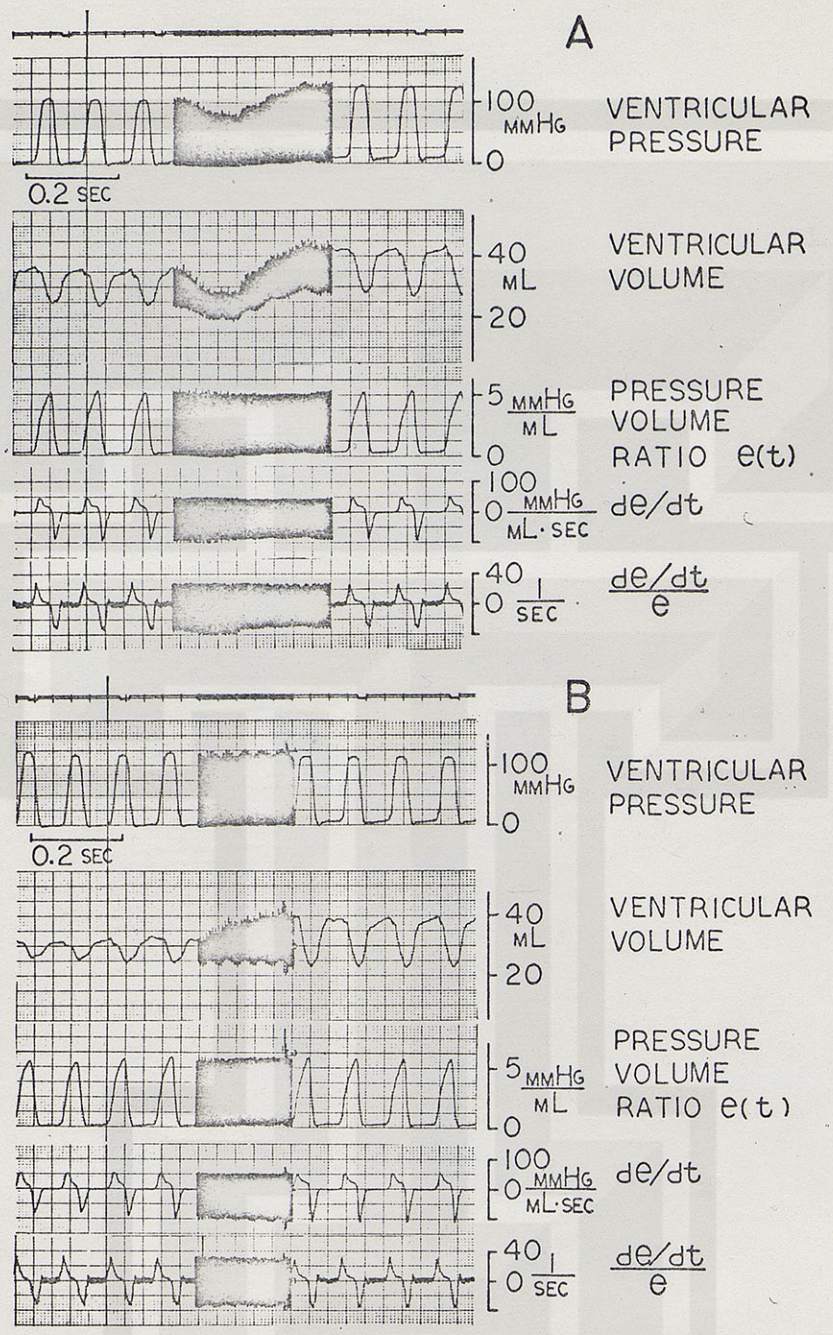

The instantaneous pressure–volume ratio curves of a canine left ventricle. The $e(t)$ curves in the third channel are computed from the intraventricular pressure (first channel) and volume (second channel). Panels A and B show the data when cardiac output was varied with and without secondary changes in mean arterial pressure, respectively. Panel C shows the relationship of $e(t)$ curves with different rates of epinephrine infusion. Panel D are the data while heart rate was varied by electrical pacing of the ventricle. In channels 4 and 5 of all the panels are the time-derivatives of $e(t)$ and $(de/dt)/e$, respectively. de/dt was computed by a CR network with a time constant of 0.5 msec and $(de/dt)/e$ was computed by an analog computer.

Figure 11 Continued

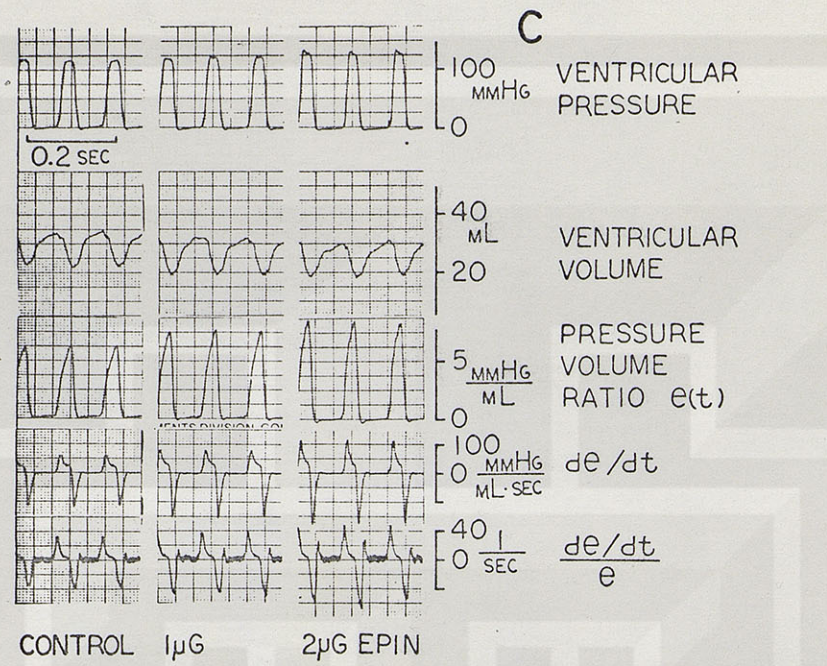

The cardiac output, or flow rate is simply the heart rate, $f = \frac{1}{T}$ multiplied by the stroke volume. Thus,

$$\dot{Q} = f(P_f{}^* C_D - P_a C_s) \quad \text{for } P_f{}^* > \frac{P_a C_s}{C_D}$$

$$\dot{Q} = 0 \quad \text{for } P_f{}^* < \frac{P_a C_s}{C_D} \qquad (2)$$

Equation (2) is plotted below. Notice that $P_f{}^*$ is measured as the transmural pressure across the ventricle, and is equal to the filling pressure P_f only in an open-chest subject.

Figure 12

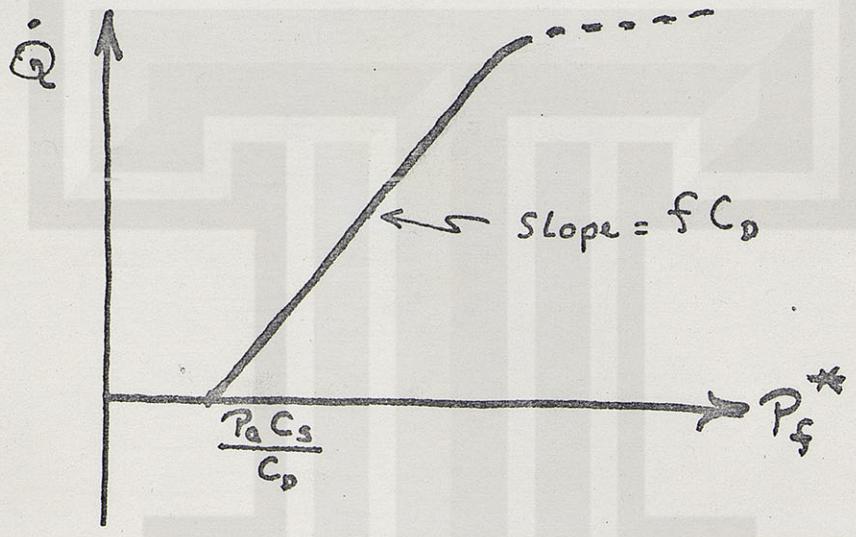

Note that the slope of the curve may be increased by increasing heart rate or diastolic capacitance. Remember also that we have assumed that there is no limit on the degree of diastolic filling--i.e., we have assumed a linear diastolic capacitance. In actual fact, of course, there are limits to the degree of diastolic filling due to collagen tissue in the heart, pericardial restriction of filling, etc. These factors will put an upper bound on cardiac output and thus we would expect "saturation effects" on the curve as shown by the dashed line.

Up to this point we have been considering a single ventricle and its behavior. It is also possible to lump together the right heart, left heart, and pulmonary circulation in a single "black box". The input is a filling pressure (right atrial pressure), and the output will be left ventricular output. The relationship between cardiac output $\dot{Q}$, and right atrial pressure, P_f, is known as a cardiac output curve, and is of the same shape as Figure 12 above. Unless otherwise noted, we will be dealing only with such lumped cardiac output curves form now on.

HEART AND CIRCULATION

Mean, Non-Pulsatile Model

Our assumption that the load pressure P_a and the filling pressure P_f are independent of each other may be valid in certain experimental conditions, but it is certainly not valid if the pump is actually connected into a circulation. In a circulation, P_a is always a function of the flow rate and the filling pressure.

$$P_a = (\dot{Q}, P_f)$$

Specifically in our model of the circulation, the relationship is given by eq. 11 on page 4 of the lecture notes. The relationship may be rewritten as:

$$P_a = \dot{Q}(R_a + R_v) + P_f \qquad (3)$$

If this constraint is added to the result of equation 2, we may obtain a relation between flow, Q, and P_f with P_a replaced by parameters describing the circulation: (assume open-chested case so $P_f^* = P_f$)

$$\dot{Q} = \frac{f(C_D - C_s)P_f^*}{1 + fC_s(R_a + R_v)} \qquad (4)$$

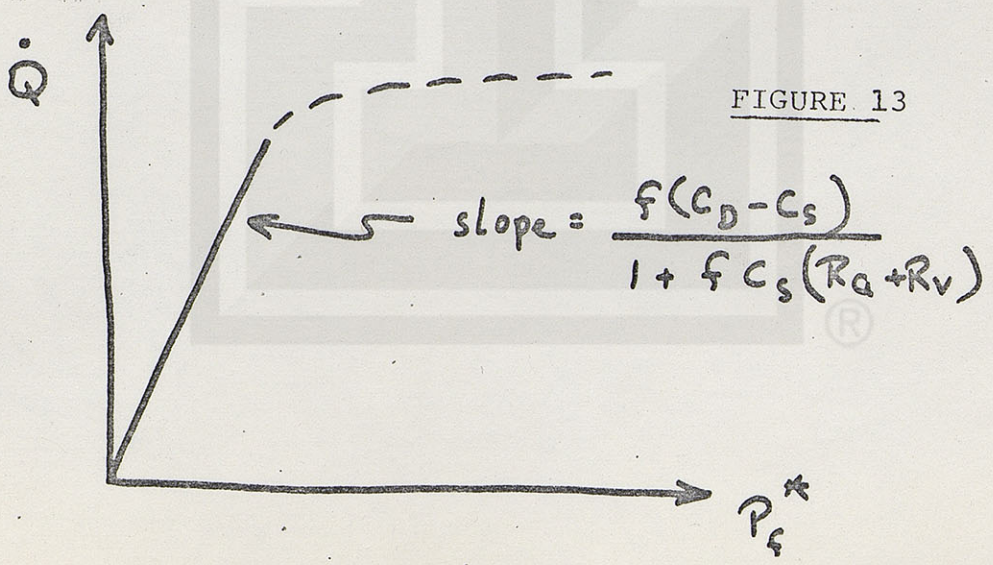

FIGURE 13

Note that the slope may be altered by changing heart rate (within limits), C_s, and the peripheral resistance. Note also the asymptotic behavior as $C_s \rightarrow 0$. Is this reasonable?

Remember that P_f^* is the transmural pressure across the pump chamber. In general, the heart is enclosed in a closed chest which is at a pressure about 5mmHg less than atmospheric.

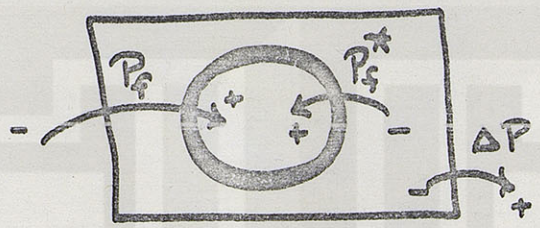

FIGURE 14

If P_f is the filling pressure referenced to atmospheric pressure,

$$P_f = P_f^* - \Delta P \tag{5}$$

If we substitute this into eq. 4, we obtain,

$$Q = \frac{f(C_D - C_s)(P_f + \Delta P)}{1 + fC_s(R_a + R_v)} \tag{6}$$

The graph of this function is identical to Figure 13 but shifted to the left by ΔP.

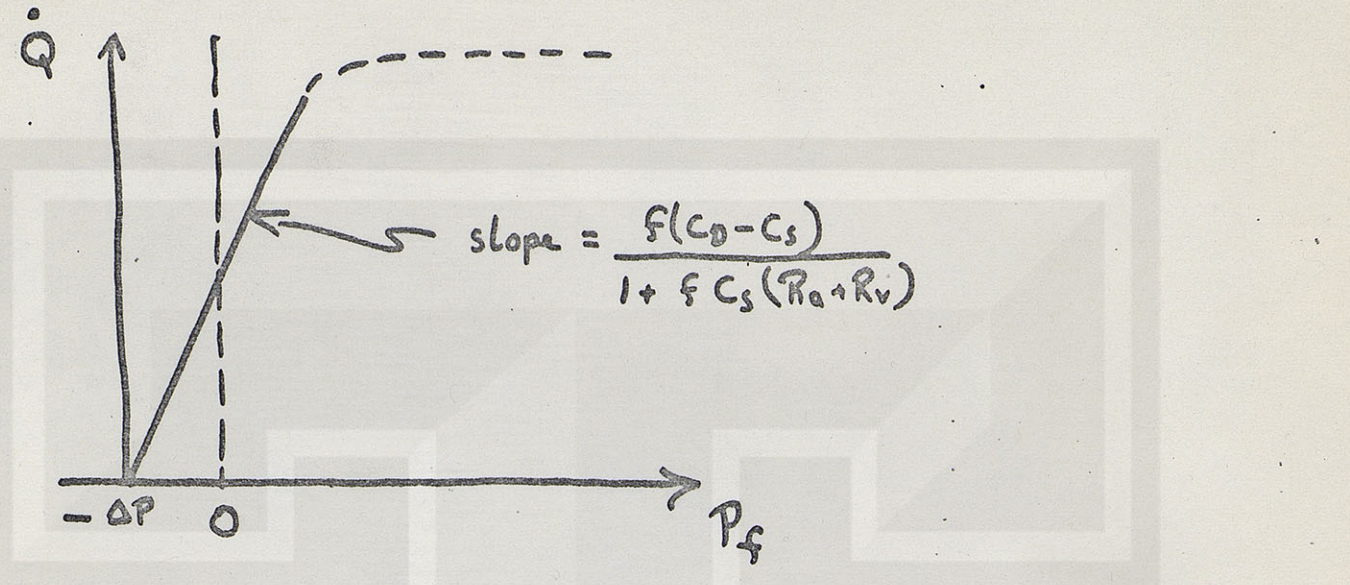

FIGURE 15

We are now ready to link the pump to the circulation and obtain a steady-state operating point. In what follows "pump" includes both right and left hearts and the pulmonary circulation.

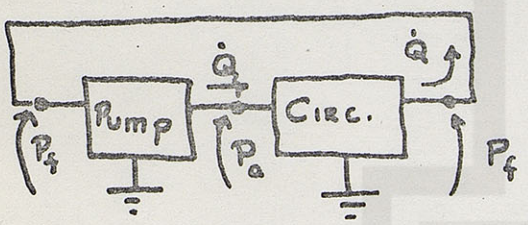

Note: 'Pump' includes both right and left hearts, and pulmonary circulation.

FIGURE 16

We have the following relationships at the input of the pump:

$$\dot{Q} = \frac{f(C_D - C_s)\ (P_f + \Delta P)}{1 + fC_s(R_a + R_V)}$$

$\dot{Q}$ is output of pump, (6)

$$\dot{Q} = \frac{P_{ms} - P_f}{R_V + \dfrac{R_a C_a}{C_a + C_v}}$$

from circulation model, with P_{ms} a fixed quantity. (vol. + C's const.) (7)

Since the $\dot{Q}$'s and P_f's are identical, we may solve the equations algebraically or graphically. The graphical technique is probably the most illuminating. The curves for eqs. 6 and 7 have been presented above.

The graphical solution is shown below:

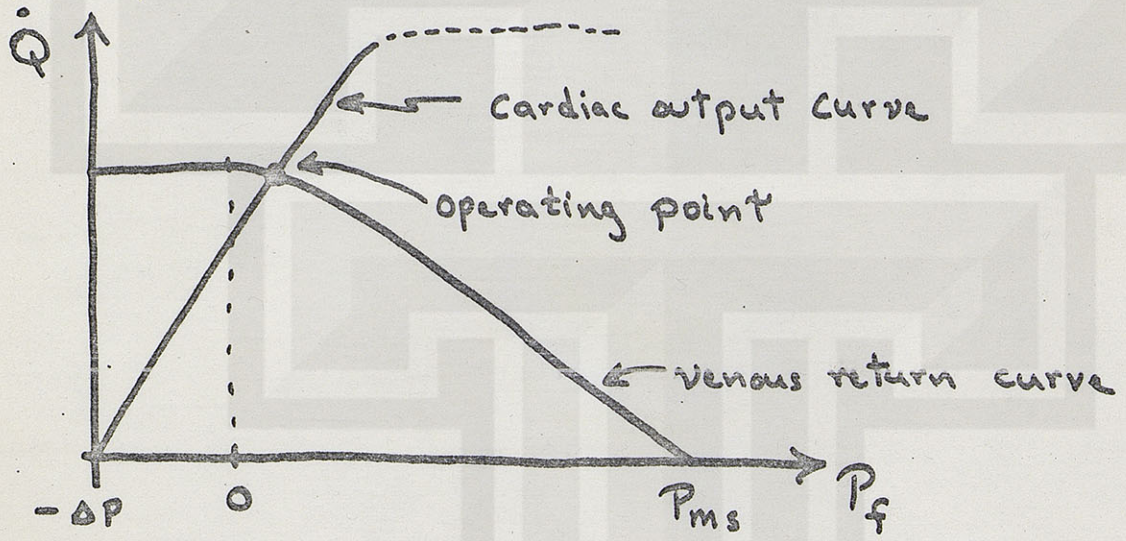

FIGURE 17

Equations 6 and 7 may be solved algebraically to obtain:

$$\dot{Q} = \frac{(P_{ms} + \Delta P) f (C_D - C_s)}{f\left[(C_D - C_s)(R_v + \beta R_a) + C_s (R_a + R_v)\right] + 1} \qquad (8)$$

where $\beta = \dfrac{C_a}{C_a + C_v}$

Equation 8 is valid only in the range of linearity of eq.'s 6 and 7. Thus, it is restricted to the region of $0 < P_f < P_f(sat)$. Nevertheless, it does serve to indicate the general direction in which $\dot{Q}$ will move in response to changing a number of system variables.

Graphical analysis of the system, as introduced by A.C. Guyton is very helpful in understanding the integrated function of the cardiovascular system. Several examples are reviewed below. Figure 18 shows normal cardiac output and venous return curves. Note that the steady state operative point is at a C.O. of 5 liters/min. and a right atrial pressure of 0 mmHg.

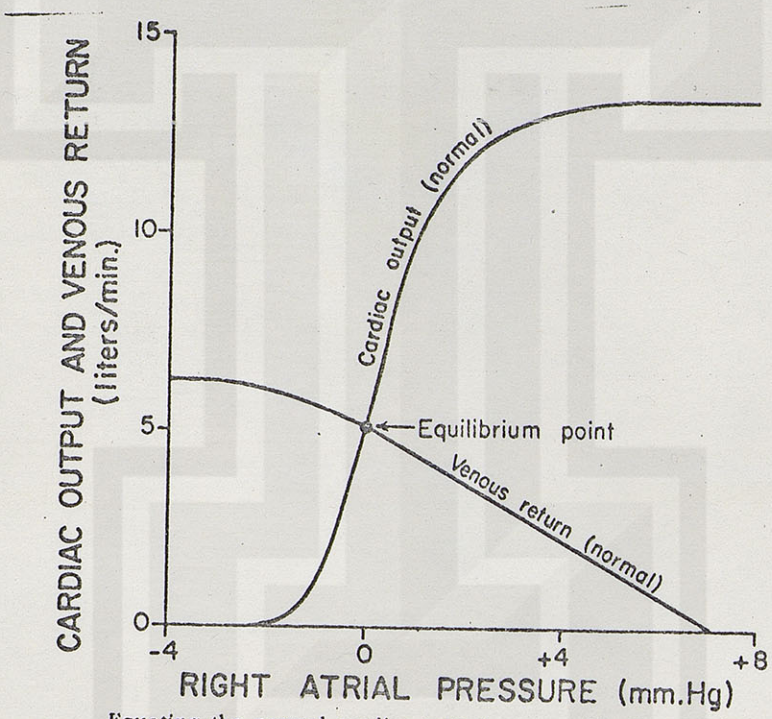

Equating the normal cardiac output curve with the normal venous return curve.

Figure 18

In the following section, we will illustrate the use of Guyton's graphical technique to analyze several specific physiological states.

A. Sympathetic Stimulation

1. Sympathetic stimulation has rather little effect on resistance to venous return, R_V.
2. Sympathetic stimulation causes constriction of veins, decreased venous capacitance, and increases mean systemic pressure--hence, moves venous return curves up and to the right.
3. Sympathetic stimulation changes the cardiac output curves by shifting to the left and increasing the slope.

Figure 19 illustrates an analysis for the combined effects of sympathetic stimulation on both cardiac and peripheral factors. The normal operating point is at "A", while with increased sympathetic tone, the operating point moves from A to C, and then to D. Notice that despite the increase in cardiac output, RA pressure drops. These curves do not show arterial blood pressure. What would you expect to happen to blood pressure under intense sympathetic stimulation?

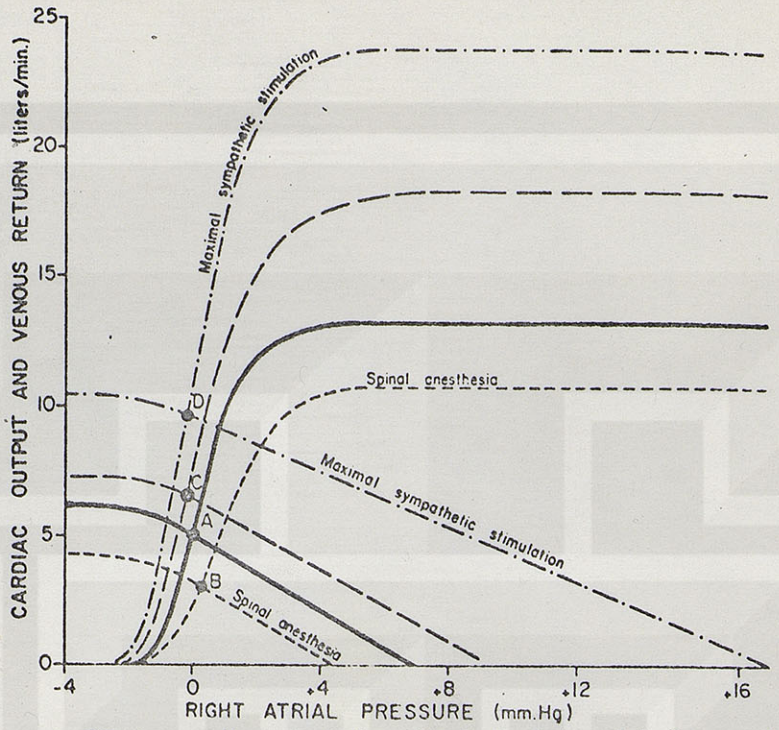

Effect on cardiac output of combined stimulation of the heart and of the peripheral vasculature, showing an increase in cardiac output of 25 per cent during moderate sympathetic stimulation, an increase of 92 per cent during maximal sympathetic stimulation, and a decrease of 40 per cent when all sympathetic tone in the body is abrogated by total spinal anesthesia.

FIGURE 19

B. Tissue Oxygen Need

Hypoxia leads to vasodilation. Thus, if a vascular bed is perfused with blood with O_2 saturation of only 30%, a prompt vasodilation is observed. Hypoxia will shift the CO curve downward and to the right--with severe hypoxia seriously damaging the heart's ability to pump. Figure 16 illustrates the graphical solution to the effect of hypoxia of two degrees on cardiac output.

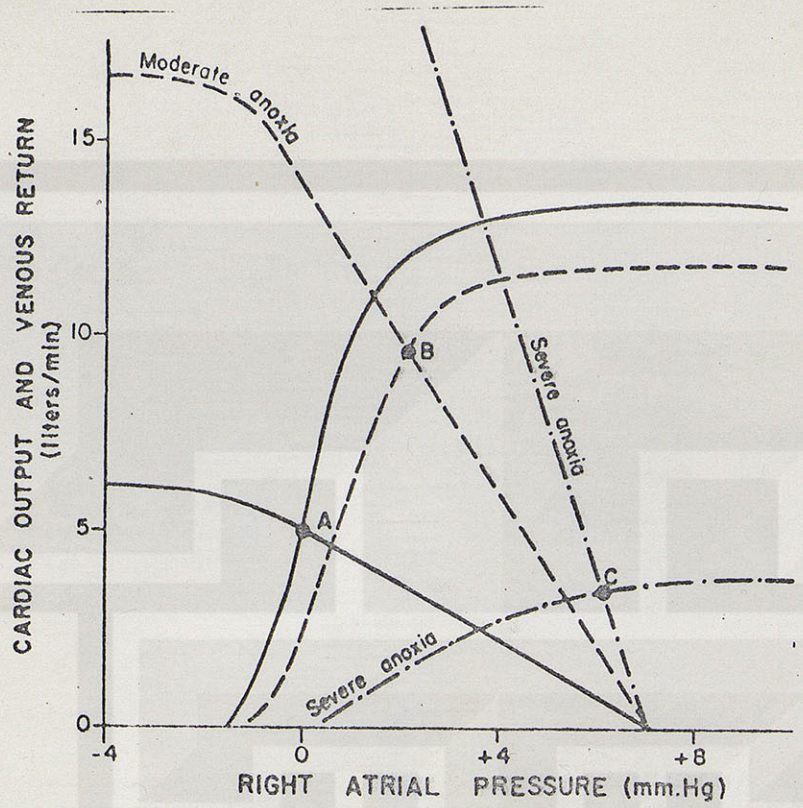

Analysis of the effect of anoxia on cardiac output. Point A represents the normal condition, point B moderate anoxia, and point C severe anoxia. See explanation in the text.

FIGURE 20

C. Muscular Exercise

The most stressful condition to the normal circulatory system is vigorous exercise. Well-trained athletes may increase their cardiac outputs by up to 6 or 7 times normal. Excercise can affect cardiac output in several ways:

1. Tensing of muscles, especially those in the abdomen and legs can increase mean systemic pressure, thus increasing venous return.
2. Autonomic stimulation may increase mean systemic pressure and also increase cardiac contractility and rate.
3. Increase in muscle metabolism causes local vasodilatation which decreases the resistance to venous return.

The time sequence of the effects are shown in Figure 21

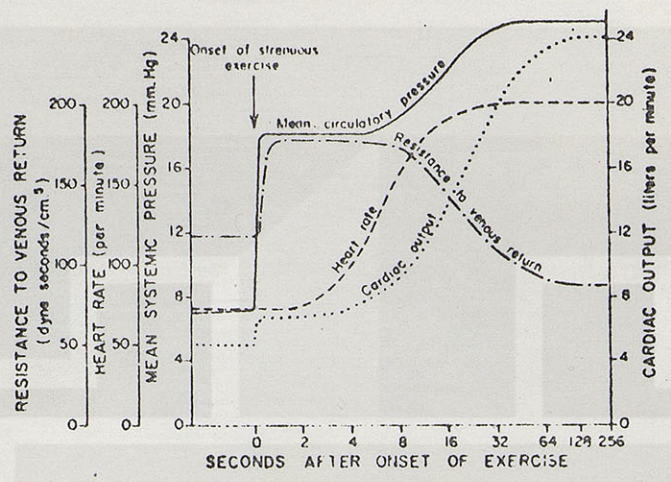

Time course of the major changes that affect cardiac output following the onset of very strenuous exercise.

FIGURE 21

The graphic analysis shown in Figure 22 illustrates the net effect on cardiac output. The normal operating point is at A. At the onset of moderate exercise, the tensing of muscles leads to an immediate increase in MSP from 7mmHg to 10mmHg, and the operating point moves to B. Note that the resistance to venous return on this venous return curve has increased slightly due to muscle clamping. The CO has increased from 5 L/min to about 6 L/min. During the next 15 to 20 seconds sympathetic stimulation becomes significant, causing both cardiac and peripheral effects. Both CO and venous return curves shift appropriately and the next operating point is at C with a cardiac output of 8 L/min at a RA pressure of 0. Finally, metabolic dilatation of the muscular vascular bed occurs, resulting in decreased resistance to venous return. The new equilibrium point at D shows a CO of 13 L/min at a RA pressure close to zero.

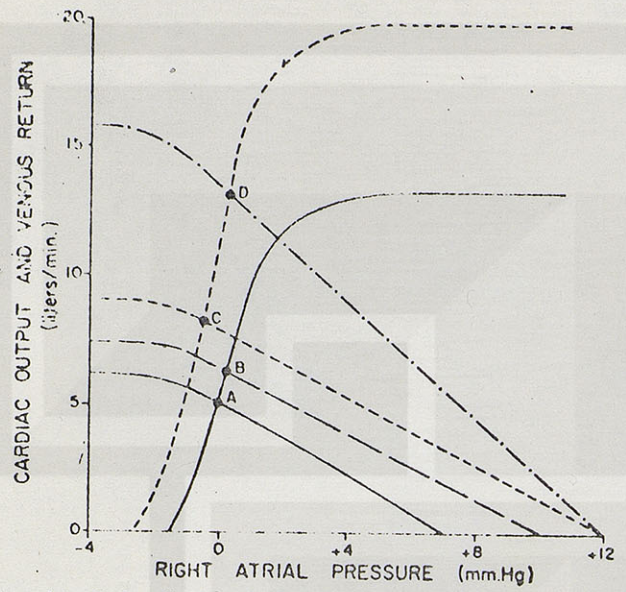

Graphical Analysis of the Effect of Moderate Exercise on Cardiac Output and Right Atrial Pressure

Graphical analysis of the changes in cardiac output and right atrial pressure at various time intervals following the onset of moderate excercise.

FIGURE 22

HOME STUDY QUESTIONS

Using the techniques discussed above, do graphical analyses for the following situations:

1. A subject is placed in a lower body negative pressure device in which his lower body is exposed to ambient pressures below atmospheric. What would happen to the venous return curves, the cardiac output curves, and the equilibrium operating point? Discuss the conditions under which fainting might occur.

2. Through graphical analysis discuss changes in cardiac output during the normal respiratory cycle.

3. Demonstrate the behavior of the cardiac output in response to the opening of a medium sized A-V fistula.

MASSACHUSETTS INSTITUTE OF TECHNOLOGY

Departments of Electrical and Mechanical Engineering

6.022J/2.792J: Quantitative Physiology: Organ Transport Systems

HEART AND CIRCULATION
Pulsatile Models

A. Impulse Generator Model

One simple pulsatile model of the heart would be a current impulse generator. Those familiar with circuit theory will recall that a current generator has infinite impedance, so valves (diodes) are not needed. A current impulse is analogous to a flow impulse and in its ideal form has infinite amplitude and infinitesimal width. Hence, it is measured by defining its area, which of course is the total charge contained in the impulse (analogous to total volume for flow impulse). Thus the current generator shown in Figure 1 becomes a heart model in which the

FIGURE 1

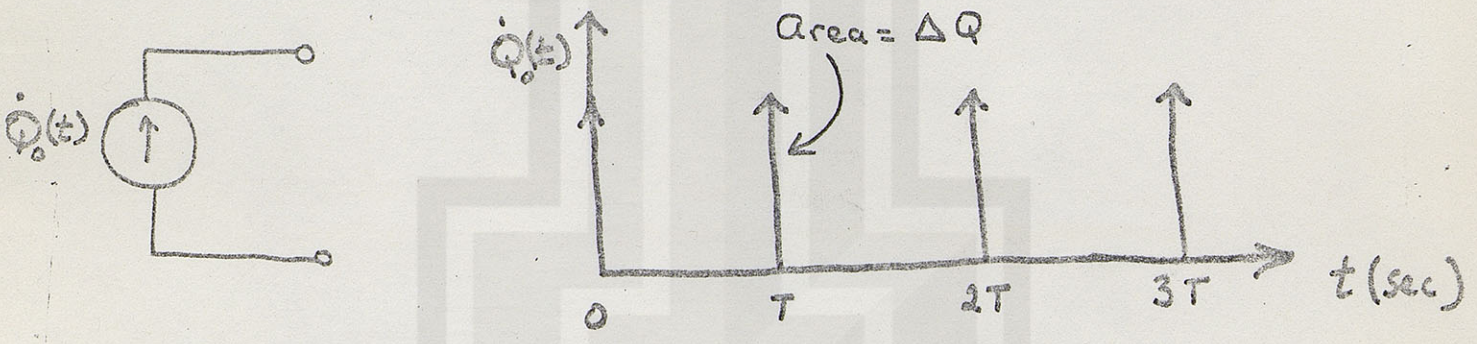

heart rate, f, is $\frac{60}{T}$ beats/min, and the stroke volume is ΔQ. What would be observed if the current generator were to be attached to a simple Windkessel model? (See Figure 2.) Note that $P_a(t)$ represents arterial pressure and $\dot{Q}(t)$, the flow.

FIGURE 2

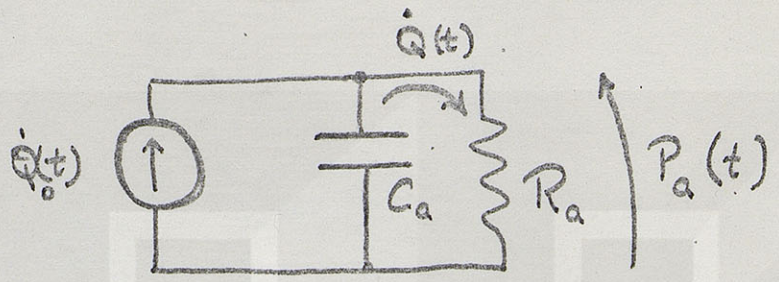

Using this model, it is possible to express the steady-state arterial pressure (systolic, diastolic, and mean) in terms of the model parameters, and to observe the dependence of these pressures on stroke volume, heart rate, arterial capacitance, and peripheral resistance. In the calculations, we will use hydraulic symbols. (Note the analogy to electrical symbols.)

$$P_a(t) = \dot{Q}(t) R_a$$

Qualitatively, the pressure waveform will appear as shown in Figure 3.

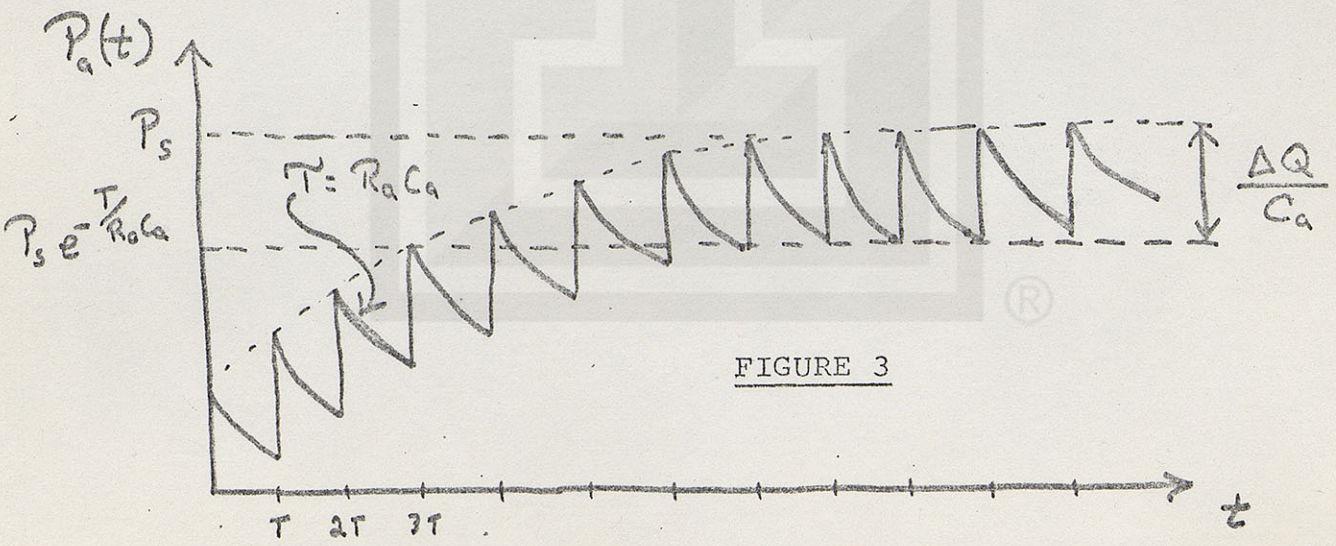

FIGURE 3

In steady state, the increment in pressure corresponding to the sudden dumping of ΔQ onto C_a will be $\frac{\Delta Q}{C_a}$. In the time T during which C_a discharges exponentially through R_a, the pressure decrease must equal $\frac{\Delta Q}{C_a}$.

If the steady-state peak pressure is P_s (systolic pressure), the minimal diastolic pressure T seconds later would be

$$P_s e^{-T/R_a C_a}$$

Hence the pressure decrease would be

$$P_s \left(1 - e^{-T/R_a C_a}\right) \qquad (2)$$

Setting this quantity equal to $\frac{\Delta Q}{C_a}$, we have:

$$P_s \left(1 - e^{T/R_a C_a}\right) = \frac{\Delta Q}{C_a} \qquad (3)$$

$$P_s = \frac{\Delta Q}{C_a} \cdot \frac{1}{(1 - e^{-T/R_a C_a})} \qquad (4)$$

During the intervals, $n\,T < t < (n + 1)T$, the expression for arterial pressure then becomes:

$$P_a(t) = \frac{\Delta Q}{C_a} \cdot \frac{1}{(1 - e^{T/R_a C_a})} e^{\frac{-(t-nT)}{R_a C_a}} \qquad (5)$$

Systolic Pressure

$$P_s = \frac{\Delta Q}{C_a} \cdot \frac{1}{(1 - e^{-T/R_a C_a})} \qquad (6)$$

Diastolic Pressure

$$P_D = \frac{\Delta Q}{C_a} \frac{e^{-T/R_a C_a}}{\left(1 - e^{-T/R_a C_a}\right)} \tag{7}$$

Pulse Pressure

$$P_s - P_d = \frac{\Delta Q}{Ca} \tag{8}$$

Mean Pressure =

$$\frac{1}{T}\int_o^T P_a(t)dt = \frac{\Delta Q}{C(1 - e^{-T/R_a C_a})}\int_o^T e^{-t/R_a C_a} dt$$

$$\overline{P_a} = \frac{\Delta Q R_a}{T} = \frac{\Delta Q f R_a}{60} \tag{9}$$

Several points are worth observing from the above expressions--first, the mean arterial pressure is directly proportional to heart rate, stroke volume, and peripheral resistance, as would be expected. Since stroke volume times heart rate equals cardiac output, equation 9 simply states that the mean arterial pressure equals the product of cardiac output and peripheral resistance.

Examination of equation 8 reveals that the pulse pressure is directly proportional to the stroke volume and inversely proportional to arterial capacitance. What does this imply for patients with severe arteriosclerotic vascular disease with pipe-like arteries?

Equation 6 shows that the systolic pressure increases with increasing R or C, and decreases as T increases.

B. Other Heart Models

The current impulse generator and Windkessel vascular model are quite useful, but have obvious limitations. The most obvious shortcoming is that only the ventricle and arterial end of the vasculature are represented, with no indication of a venous return or real circulation of blood.

A somewhat more complicated heart model is necessary to account for these factors. In general block form, the heart model must contain the inlet and outlet valves, and a pumping chamber (Figure 4).

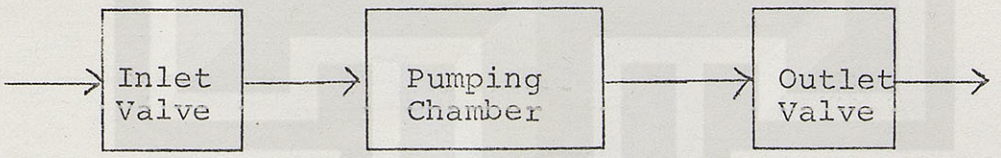

FIGURE 4

Our variable capacitor model, discussed previously, fits this form and we may examine its pulsatile behavior when driving the Windkessel vasculature model, and being supplied by a constant venous pressure source (Figure 5).

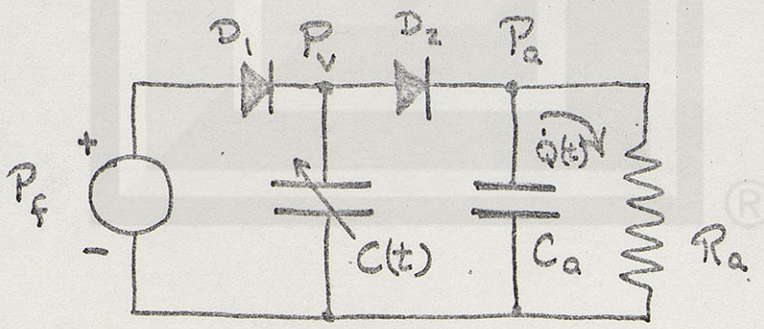

FIGURE 5

In analyzing the steady-state behavior of this model, we will begin with diastole. We will adopt the following definitions:

C_s = ventricular capacitance during systole
C_d = ventricular capacitance during diastole
C_a = arterial capacitance
R_a = peripheral resistance
P_f = venous pressure = filling pressure
P_v = ventricular pressure
P_a = arterial pressure
Subscript 's' denotes systole,
Subscript 'd' denotes diastole
Superscript 'o' denotes beginning of period
Superscript 'e' denotes end of period.

During diastole, the circuit becomes simplified because D_2 opens (ventricular pressure drops as $C_s \longrightarrow C_d$) (Figure 6). Clearly, C_d will be filled to a pressure, P_f,

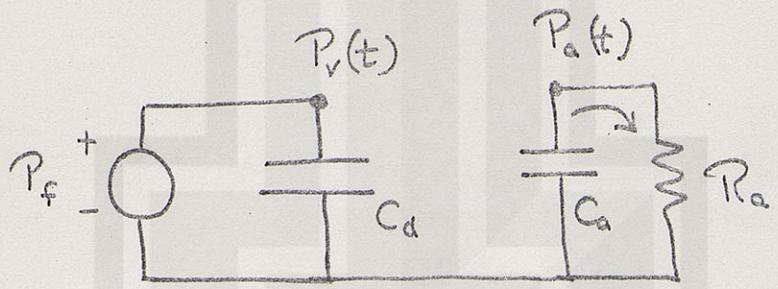

FIGURE 6

and will instantly accumulate a total end-diastolic volume of $C_d P_f$. At the same time, during diastole an exponential

decay will occur in the arterial pressure $P_a(t)$ (Figure 7); with a time constant $\tau_d = C_a R_a$.

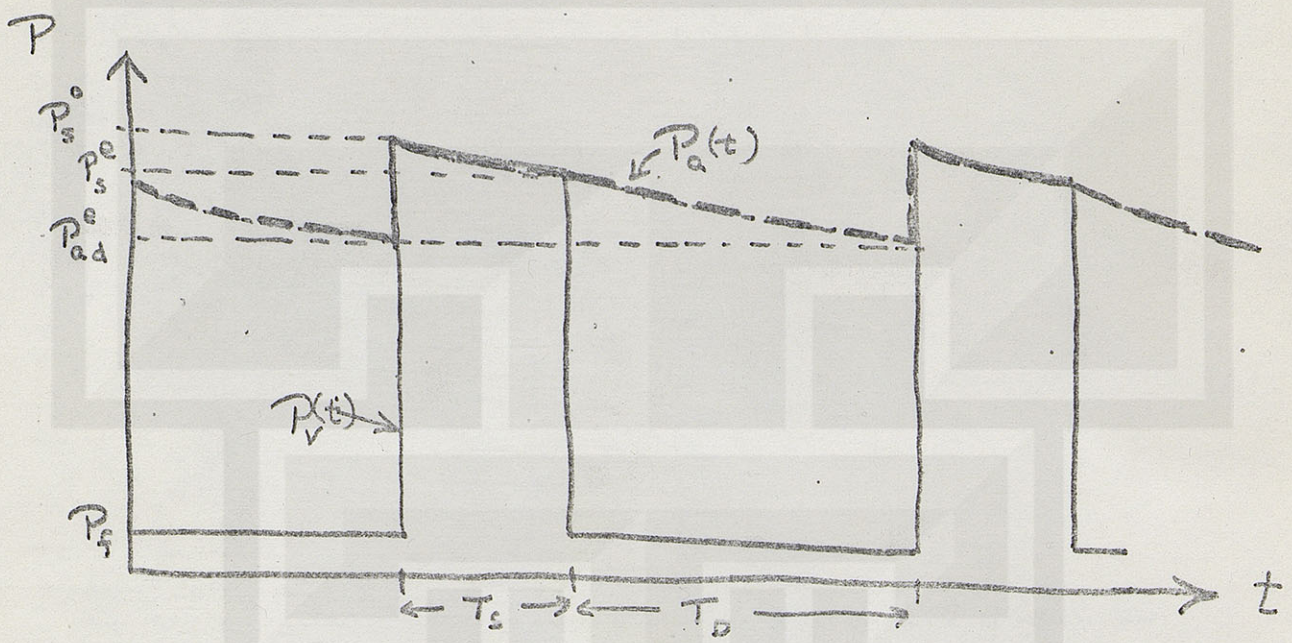

FIGURE 7

At the onset of systole, C_d decreases to C_s. Note that this transformation involves work, and external energy is required. How much?* The pressure $P_v(t)$ will suddenly increase since volume does not change instantly. This increase in $P_v(t)$ will open D_1 and close D_2, so the circuit in systole will be as shown in Figure 8. Now $P_{vs}(t)$ must equal $P_{as}(t)$ and volume will transfer from C_s to C_a to make this possible. The value of $P_{vs}(t)$ at the onset of systole is P^o_{vs}. The volume in C_s will be $P^o_{vs}C_s$ and the volume in C_a will be $P^o_{vs}C_a$. The original volume on C_s at

*Answer: $\Delta W = \frac{Q^2}{2}\left(\frac{1}{C_s} - \frac{1}{C_d}\right)$

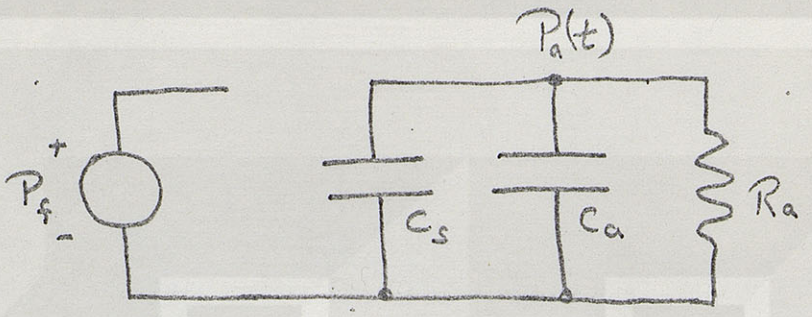

FIGURE 8

at end-diastole was $C_d P_f$, while the end-diastolic volume in C_a was $C_a P^e_{ad}$. By conservation of mass, it follows that:

$$P^o_{vs}(C_s + C_a) = C_d P_f + C_a P^e_{ad}$$

$$P^o_{vs} = \frac{C_d P_f + C_a P^e_{ad}}{C_s + C_a} \qquad (10)$$

Throughout the duration of systole, T_s, the pressure $P_{vs}(t) = P_{as}(t) \cong P_s(t)$, and hence the RC time constant is

$\tau_s = R_a(C_s + C_a)$.

The pressure at the end of systole, P^e_s is:

$$P^e_s = P^o_s e^{-T_s/\tau_s} \qquad (11)$$

The volume on C_s at the end of systole is therefore

$$Q^e_s = P^o_s C_s e^{-T_s/\tau_s} \qquad (12)$$

The pressure $V_a(t)$ decays during diastole with a time constant $\tau_d = R_a C_a$, and hence the pressure at the end of diastole becomes

$$P^e_{ad} = P^o_{ad} e^{-T_d/\tau_d}$$

$$= P^e_{as} e^{-T_d/\tau_d}$$

$$= P^o_s e^{-T_s/\tau_s} e^{-T_d/\tau_d} \qquad (13)$$

Where T_d is the duration of diastole.

Combining eq.13 and eq. 10, we may relate the peak systolic pressure P^o_{vs} to the end diastolic ventricular pressure P_f directly.

$$P^o_s = \frac{C_d P_f}{C_s + C_a} + \frac{C_a}{C_s + C_a} P^o_s e^{-\left[\frac{T_s}{\tau_s} + \frac{T_d}{\tau_d}\right]}$$

$$P^o_s \left[(C_s + C_a) - C_a e^{-\left(\frac{T_s}{\tau_s} + \frac{T_d}{\tau_d}\right)}\right] = C_d P_f$$

$$P^o_s = \frac{C_d P_f}{C_s + C_a \left[1 - e^{-\left(\frac{T_s}{\tau_s} + \frac{T_d}{\tau_d}\right)}\right]} \qquad (14)$$

The "Stroke Volume" is equivalent to the net transfer of volume from the ventricle between end-diastole and end-systole.

Thus,

Stroke Volume = ΔQ = Q (end Diastole) - Q (end systole).

$$\Delta Q = C_d P_f - C_s P_s^o e^{-\frac{T_s}{\tau_s}}$$

Substituting from eq. 14, this becomes

$$\Delta Q = C_d P_f - \frac{C_d C_s e^{-\frac{T_s}{\tau_s}} P_f}{C_s + C_a \left[1 - e^{-\left(\frac{T_s}{\tau_s} + \frac{T_d}{\tau_d}\right)}\right]}$$

$$= C_d P_f \left\{ \frac{C_s + C_a (1-e^{-k}) - C_s e^{-\frac{T_s}{\tau_s}}}{C_s + C_a (1-e^{-k})} \right\}$$

where $k \equiv \frac{T_s}{\tau_s} + \frac{T_d}{\tau_d}$

$$\Delta Q = C_d P_f \left\{ \frac{C_s (1-e^{-\frac{T_s}{\tau_s}}) + C_a \left[1-e^{-\left(\frac{T_s}{\tau_s} + \frac{T_d}{\tau_d}\right)}\right]}{C_s + C_a \left[1-e^{-\left(\frac{T_s}{\tau_s} + \frac{T_d}{\tau_d}\right)}\right]} \right\} \quad (15)$$

Notice that for constant C's, T's and τ's the stroke volume becomes proportional to P_f, the ventricular diastolic pressure.

Stroke volume increases as the diastolic capacity C_d increases, which agrees with our intuition. Furthermore, the stroke volume increases as the systolic ventricular capacitance decreases (ventricle empties more), until as $C_s \rightarrow o$ we have

$$\Delta Q = C_d P_f$$

This simply states that when the ventricle empties completely, the stroke volume must equal the end-diastolic volume. (This is identical with equation (1) of notes for lecture 6 when $C_s \rightarrow o$.)

These relationships are plotted qualitatively in Figure 9, and resemble the familiar Starling-type ventricular function curves. These curves, too, are similar to those derived for the model above.

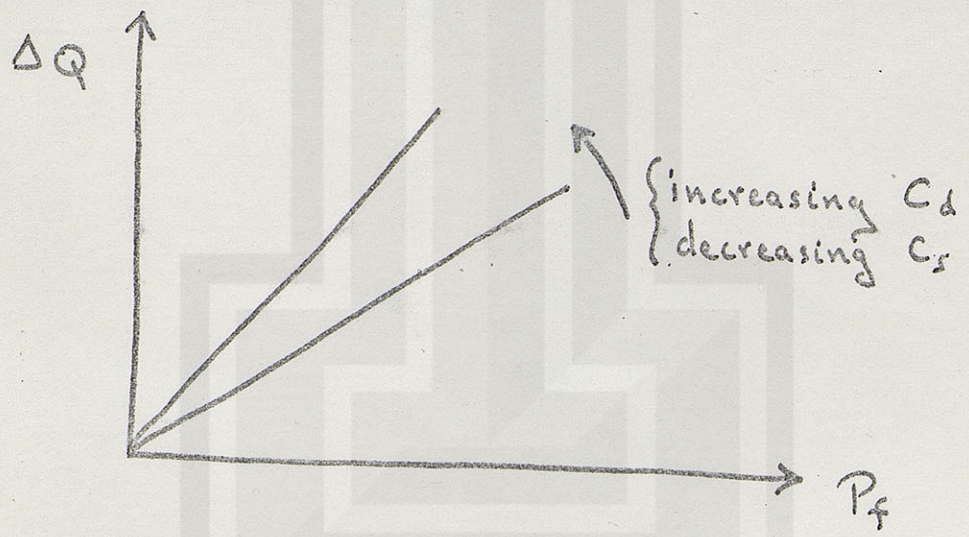

FIGURE 9

Having familiarized ourselves with how the heart model works with a constant venous pressure and a Windkessel vasculature, we may move on to a more complete model which includes the entire circulation. (Figure 10.)

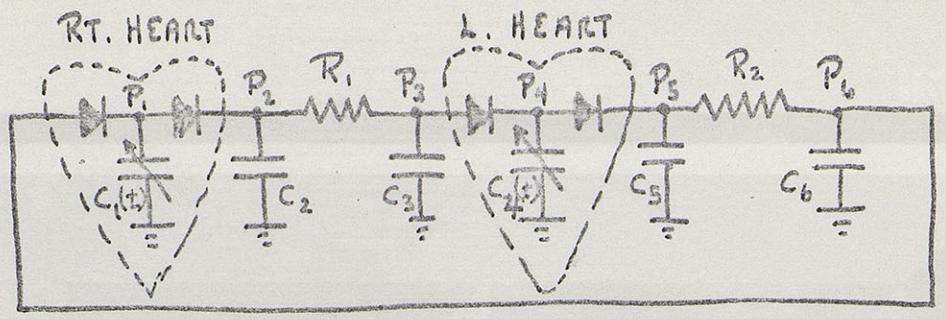

FIGURE 10

MASSACHUSETTS INSTITUTE OF TECHNOLOGY

Departments of Electrical and Mechanical Engineering

PROBLEM SET #2 2.792J/6.792J

Problem #1

The continuity and momentum equations for a frictionless fluid in a pipe (artery) were presented in class:

$$\text{Continuity} \qquad \frac{\partial Q}{\partial x} + \frac{\partial A}{\partial t} = 0$$

$$\text{Momentum} \qquad \frac{\partial v}{\partial t} + v \frac{\partial v}{\partial x} = -\frac{1}{\rho} \frac{\partial p}{\partial x}$$

$$v = Q/A$$

a) By substituting $v = Q/A$ in the momentum equation and using the continuity equation, show that the momentum equation can be written

$$\frac{\partial Q}{\partial t} + \frac{\partial}{\partial x}\left(\frac{Q^2}{A}\right) = -\frac{A}{\rho} \frac{\partial p}{\partial x}$$

b) Estimate the ratio

$$R \equiv \frac{\frac{\partial}{\partial x}\left(\frac{Q^2}{A}\right)}{\frac{\partial Q}{\partial t}} \approx \frac{\frac{1}{\Delta L}\left(\frac{Q^2}{A}\right)}{\frac{1}{\Delta t}(Q)}$$

for the aorta using $\Delta t \cong 1$ a heart period and ΔL equal to the length of the aorta. Can the term

$$\frac{\partial}{\partial x}\left(\frac{Q^2}{A}\right)$$

be neglected as small?

c) Discuss why the numerical value R estimated in (b) might be too high.

Problem #2

The results of both the Wormsley theory for pulsatile flow in a tube and the simpler Rayleigh problem for oscillating flow over a flat plate lead to the same conclusion: for $\alpha = \sqrt{\omega/\nu} \gg 1$, the thickness of the viscous layer near the artery wall is very thin, and the thickness, δ, is independent of tube radius, i.e.

$$\delta \approx \sqrt{2\omega/\nu}$$

a) We wish to apply this result in estimating the wall shear stress in a branching artery. The wall shear stress

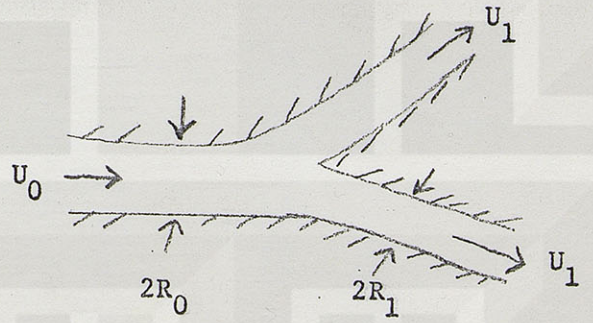

in each vessel is

$$\tau_{wall} = \mu\left(\frac{\partial u}{\partial r}\right)_{wall} \approx -\mu\frac{U}{\delta}$$

where U is the velocity in the vessel and δ is the viscous layer thickness. Determine the parent-daughter shear ratio for a symmetric bifurcation:

$$K \equiv \frac{\tau_0}{\tau_1}$$

Is K generally greater or less than 1 in the major human arteries?

b) If we used the model of Poiseuille flow,

$$u(r) = \frac{2Q}{\pi R^2}(1 - r^2/R^2)$$

a different scaling result would be obtained. Compute K as a function of the radius ratio (R_1/R_0) for a symmetric bifurcation using the model of Poiseuille flow.

Problem #3

In Exercise 1 above, you derived the following form of the momentum equation for an inviscid fluid:

$$\frac{\partial Q}{\partial t} + \frac{\partial}{\partial x}\left(\frac{Q^2}{A}\right) = -\frac{A}{\rho}\frac{\partial p}{\partial x}$$

Here, $A = A(p,x)$, and is given by the compliance

$$Cu = \frac{\partial A}{\partial p} \approx \text{constant or}$$

$$A = Cu(p - p_{ref.})$$

a) Integrate the momentum equation from $x = 0$ (the root of the vessel) to its terminal end at $x = L$, and obtain

$$p_0 - p_L\left(\frac{A_L}{A_0}\right) = \frac{\rho L}{A}\left[\overline{\left(\frac{\partial Q}{\partial t}\right)} + \frac{1}{L}\left(\frac{Q^2}{A}\right) - \frac{1}{L}\left(\frac{Q^2}{A}\right)_0\right]$$

where $\overline{(\partial Q/\partial t)}$ is the average acceleration of the fluid along the length of the vessel.

b) The quantity $(\rho L/A)$ is called the inertance of the fluid, $\mathcal{L}$, and is analogous to an inductor in an electrical circuit. Justify this interpretation by considering the case where A and Q are nearly constant along the vessel length.

Problem #4

Discuss, using the cardiac output and venous return graphs the events which occur in the cardiovascular system of a healthy man following a 1000cc. blood loss. Include all of the control mechanisms with which you are familiar.

Problem #5

Show, using the graphic technique, the expected sequence of cardiovascular events during cyanide poisoning (a form of asphyxia).

Problem #6

Assume wave propogation in the arterial tree to be adequately modeled by the transmission line with constant parameters. Consider a symmetric arterial bifurcation such as the iliac bifurcation. What must be the required geometric relationships between parent and daughter vessels for no reflections to take place? (Assume modulus of elasticity does not change across the bifurcation), and also assume $C_u \approx \frac{2\pi r^3}{Eh}$

MASSACHUSETTS INSTITUTE OF TECHNOLOGY

Department of Mechanical and Electrical Engineering

2.792J/6.022J Quantitative Physiology: Organ Transport Systems

FLOW IN THE MICROCIRCULATION

Although the ancient Greeks were familiar with the anatomy of the heart and major blood vessels, the concept of a closed circuit for the circulation was not firmly established until the early 17th Century. Later in that century, and continuing into the early 19th Century, some ingenious experiments were conducted in an attempt to isolate the major sources of resistance to flow. It is a credit to the investigators of that time, particularly Thomas Young (1808-1809), that they succeeded in establishing that the major resistance to flow occurred in vessels whose diameter was some small multiple of the size of a red cell. The experiments of Hagen (1839) and Poiseuille (1840) were performed in an attempt to elucidate the flow resistance of the human microcirculation.

In the last two decades, major strides have been made in understanding the detailed fluid mechanics of the microcirculation. While an undergraduate course in organ physiology is certainly not an appropriate point to review all of these developments in detail, we have every opportunity to extract from these studies a concrete picture of the flow in capillaries and other small vessels. Two contemporary review articles, with style as well as extensive bibliographies, are highly recommended to the interested student; they are:

> -- Richard Skalak, "Mechanics of the microcirculation", in Biomechanics, Its Foundations and Objectives, (Y.C. Fung, N. Perrone, and M. Anliker, Eds.), Prentice-Hall, Englewood Cliffs, N.J. (1972), Ch. 18.
>
> -- J.M. Fitz-Gerald, "The mechanics of capillary blood flow," in Cardiovascular Fluid Dynamics, Vol. 2, (D.H. Bergel, Ed.) Academic Press, N.Y. (1972), Ch. 16.

A. Structure of the Microcirculation

We include in the term "microcirculation" those vessels with lumens (internal diameters) which are some modest multiple -- say 1 to 10 -- of the major diameter of the unstressed red cell. This definition includes primarily the arterioles, the capillaries, and the post-capillary venules. The capillaries are of particular interest because they are generally from 6-10μ in diameter, i.e. about the same size as the red blood cells (RBC). In contrast to the larger vessels, where RBC may tumble and interact with one another and move from streamline to streamline as they course down the

vessel, the RBC must travel in single file through true capillaries. Clearly, any attempt to adequately describe the behavior of capillary flow must recognize the particulate nature of the blood.

The architecture of the microcirculation is very complex, with many parallel branches between the arterial and venous vessels. Figure 1 illustrates the tortuous route which the blood must traverse through the capillary bed. The schematized pathway of this figure will be illustrated by a movie provided by Dr. H.J. Berman of Boston University, in which the in vivo flow of blood through the hampster cheek pouch is recorded.

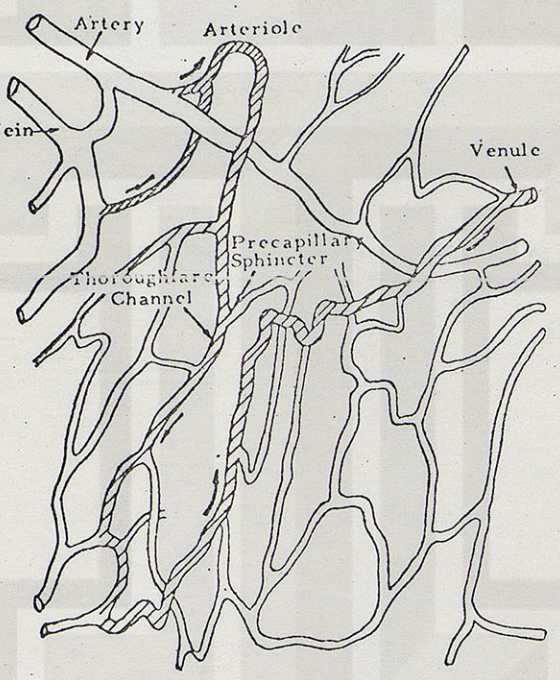

Fig. 1 Typical "architecture" of the microvasculature. (After B.W. Zweifach, Functional Behavior of the Microcirculation, C.C. Thomas, Publ., Springfield, Ill., 1961).

In addition to the elaborate vessel architecture, there is a second important feature of capillary flow; motion in any particular vessel is highly erratic, stopping and starting in an erratic and apparently random manner. The motion is not random, however, as it is controlled by the oxygen demand of the tissue which is being served by the capillary. As illustrated in Fig. 1, there are small muscular sphincters located at the

terminae of the arterioles which control the flow through the capillaries. A simplified model for this control can be given as follows: the closure of the sphincter requires oxygen to sustain tension in the musculature. As the oxygen supply in the tissue surrounding the sphincter becomes depleted, the muscles cannot sustain their tension and the vessel begins to open. But "Laplace's law" tells us that as the diameter increases, the wall tension must also increase to balance the increased internal pressure force acting against the increased wall area ($T = Rp$). The relaxed muscle cannot withstand this tension, and opens rapidly until the tension is accommodated by non-muscular tensile members in the vessel wall which limit the maximum sphincter diameter. As the musculature regains its load-carrying ability by virtue of the new supply of oxygen delivered by the flowing blood, its contractile force exceeds the tension in the arteriole wall and, again by Laplace's law, finds that the stable state is that for which the sphincter is closed. This "bang-bang" control model, while somewhat speculative, is consistent with in vivo observations.

B. A Simplified Model of Capillary Flow

The tortuosity and intermittency of capillary flow argue strongly that the case for an analytic description is lost from the outset. To prove this, we must return to the Navier-Stokes equations for a moment and compare the various acceleration and force terms which apply in the microcirculation. The momentum equation, which is Newton's second law for a fluid, can be written

(A) (B) (C) (D)

$$\rho \frac{\partial \vec{v}}{\partial t} + \rho(\vec{v} \cdot \nabla)\vec{v} = -\nabla p + (\text{viscous shear force}) \qquad (1)$$

(Forces other than the two given may be neglected.) Since we are analyzing capillaries in which the RBC are considered solid bodies travelling in a tube and surrounded by a water-like fluid (plasma), a good representation of the shear forces acting in the fluid phase is the Newtonian flow

$$\text{viscous shear force} = \mu \nabla^2 \vec{v} \qquad (2)$$

We now examine the four terms in the momentum equation from the vantage point of an observer sitting on the erythrocytes. It is an observable fact that most frequently the fluid in the capillary moves at least 10-20 vessel diameters before flow ceases, so that a characteristic time for the unsteady term (A) is, say, 10 D/U. The distance over which the velocity varies by U is, typically, D. (In the gap between the RBC and the wall, this distance is, of course, smaller but the sense of our

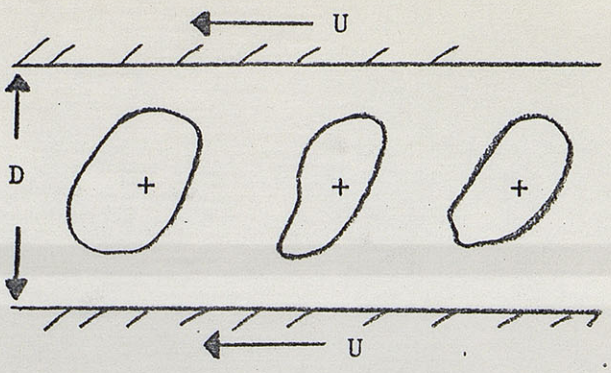

Fig. 2. Capillary flow as seen from a coordinate system in which the erythrocytes are stationary.

argument is not changed.) Dividing both sides of Eq. (1) by ρ, and defining the kinematic viscosity, ν, to be equal to (μ/ρ), we have the following order-of-magnitude comparisons between terms:

$$\frac{(A)}{(D)} \sim \frac{U/(10D/U)}{(\nu U/D^2)} = \frac{UD}{10\nu}$$

$$\frac{(B)}{(D)} \sim \frac{U^2/D}{(\nu U/D^2)} = \frac{UD}{\nu}$$

The term UD/ν is, of course, the Reynolds number. Typical values for human capillaries are $U \sim 500\mu$/sec., $D \sim 7\mu$, ν(plasma) $\sim 1.5 \times 10^{-2}$ cm^2/sec., so that the Reynolds number is about 2×10^{-3}. Clearly, the unsteady and convective acceleration terms* are negligible compared to the viscous forces.

This result is most welcome, because it allows us to neglect the acceleration of the fluid as it passes around and between the RBC, and establish a continuous balance between the local net pressure force acting on an element of fluid and the viscous stresses acting on the same fluid element. The equation to be solved, then, is

$$\nabla p = \mu \nabla^2 \vec{v}$$

*See the Appendix.

subject to the condition that the fluid velocity is zero at the erythrocyte surface, which is our fixed frame of reference, and U at the capillary wall. We must also place boundary conditions on both the pressure and velocity at the tube ends, and specify the actual shape and distribution of the red cells. This requires some drastic simplifications if we wish to obtain quantitative results, so we assume that the red cells all have a uniform shape (sphere, disc, ellipse, pancake, etc.) and are spaced at regular intervals. Then the flow, and hence the pressure, will also be subject to the requirement of periodicity, and we can idealize the ends of the capillary as being substantially removed from the region being analyzed. If we specify the relative velocity U between the capillary and the RBC, the total pressure drop across the capillary may be computed.

C. Results of the Calculation

For isolated and modestly-spaced RBC, the results of the calculation are not especially surprising. Figure 3 is a diagram of the fluid velocities in the vicinity of the red cell. In the gap, the velocity

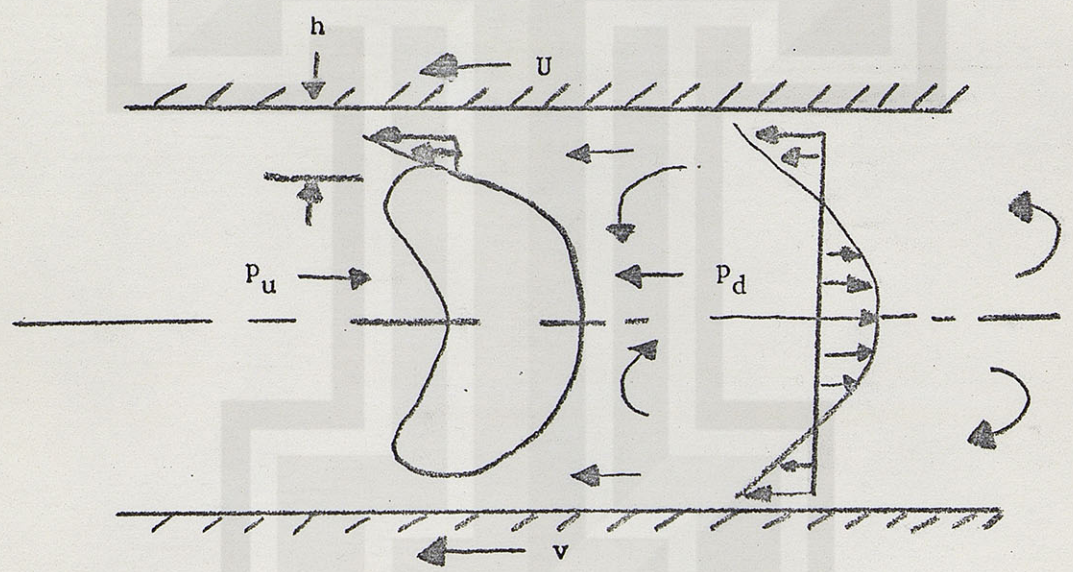

Fig. 3. Diagram of the fluid velocities near the red cell.

varies from U to zero in a distance h , whereas in the "bolus" region between the RBC, the same variation is achieved over a distance of (D/4). If $h < (D/4)$, as is often observed in vivo, then the viscous shear force is greatest in the gap region and tends to "pull" the RBC along in the direction of relative motion of the wall. Counteracting this viscous force

must be a net pressure, $p_u - p_d$, acting in a direction opposite to the sense of the shear force. This balance of forces is the origin of the parachute-like shape shown in Fig. 3 and frequently observed under a microscope.

For $h << (D/4)$, we have very roughly

$$(p_u - p_d) \cdot \frac{\pi D^2}{4} \approx (\mu \frac{U}{h}) \cdot (\pi D) \cdot (2b) \qquad (4)$$

where $2b$ is the axial extent of the region of the gap. Suppose we use Eq. (4) to estimate the pressure drop across a typical capillary. If we take $h = .02D$, $b = 0.1D$ $U = 500\mu$/sec, $D = 7\mu$, and $\mu = 1.4 \times 10^{-2}$ dyne-sec/cm^2, then

$$p_u - p_d \approx 8\mu \left(\frac{U}{h}\right)\left(\frac{b}{D}\right)$$

$$= 40 \text{ dynes/cm}^2$$

For a capillary bed of effective length 1mm, and assuming the fairly close spacing of red cells of 2μ to achieve physiological hematocrits, the overall capillary pressure drop is

$$\Delta p = (p_u - p_d) \times \frac{1000\mu}{2\mu}$$

$$\approx 40 \times 500 = 20{,}000 \text{ dynes/cm}^2$$

$$\approx 15 \text{ mm Hg.}$$

It has been estimated by several investigators that between 20 and 30% of the systemic pressure drop occurs across the capillaries, i.e. the total capillary pressure drop should be 20 - 30 mm Hg. Thus, the crude calculation of Eq. (4) is within a factor of 2 of the correct result. Note well, however, that in order to get reasonable agreement, we picked a very small value for h, (h/D) = 0.02. We conclude that the gap between the red cell and the capillary wall must be small indeed, if we are to predict correctly the overall pressure drop across the capillary. By comparison, a fully-developed Poiseuille flow gives

$$\Delta p = 32\mu \left(\frac{\bar{U}}{D}\right) \cdot \left(\frac{L}{D}\right)$$

and taking the values for L, $\bar{U}$ and D from the preceding example, but a viscosity characteristic of the average bulk blood of 4×10^{-2} dyne-sec/cm^2, we calculate a pressure drop of only 12 mm Hg. Thus, the discrete nature of the RBC leads to an increased resistance to flow.

D. Bolus Flow

As illustrated in Fig. 3, the fluid in the bolus region between red cells tends to exhibit a velocity in the retrograde, or reverse direction relative to the coordinate system fixed to the erythrocyte. Viewed from a reference frame fixed to the capillary wall, the plasma along the axis would be travelling along the tube at a velocity higher than that of the RBC. At first this might be somewhat counter-intuitive, but it is easily explained if we imagine that the RBC fit tightly in the tube [$(h/D) \to 0$] and view the resulting motion from the vantage point of the RBC.

As the wall moves axially from one erythrocyte towards the next, the fluid in the vicinity of the wall will be set into motion in the direction of the wall movement. But with $(h/D) \to 0$, there is negligible "leak-back" through the gap, and the fluid within the bolus must therefore recirculate continuously in a ball-bearing-type circulatory motion. This is indicated by the curved direction arrows in Fig. 3. For large separations between erythrocytes, the velocity profile is parabolic (like Poiseuille flow), and the retrograde velocity along the axis is exactly equal to the relative wall velocity U. If the separation between RBC is small, more complicated recirculation patterns result.

E. Viscosity of Blood

As time permits, the following topics will be discussed:

1. Non-Newtonian behavior of blood at low shear rates.
2. Agglomeration as observed in the microvasculature.
3. The Fahraeus-Lindqvist effect
    a) Reduced hematocrit in small tubes
    b) Apparent decrease of viscosity in flow through small tubes.

APPENDIX. NOTE ON CONVECTIVE ACCELERATION

Several times the question has been posed, "What is the origin of, and physical meaning of, the so-called convective acceleration term in the Navier-Stokes equations?" This note is intended as a quick and dirty physical explanation to this question.

When we write the equation for conservation of momentum of a fluid, we are simply expressing Newton's second law:

Rate of change of momentum = $\sum$ forces acting on the particle

To apply this law, we must adopt a coordinate system moving with the fluid so that we may properly evaluate its change in momentum.

Writing Newton's second law for a fluid is most conveniently accomplished by dealing with the mass per unit volume and the forces per unit volume. For incompressible fluids such as water and blood, we express the mass per unit volume as a constant density, ρ . Then the rate of change of momentum per unit volume <u>following the fluid</u> is

$$\frac{D}{Dt}(\rho \vec{v}) = \rho \frac{\vec{Dv}}{Dt}$$

$$= \sum \text{Forces per unit volume.}$$

The term $(\vec{Dv}/Dt)$ represents the total acceleration of the fluid in fluid-fixed coordinates. But it is frequently easier to solve a problem (and specify the forces acting) if we adopt a stationary coordinate system through which the particle moves. The total acceleration in the fixed coordinate system then has two distinct parts. The first represents the rate of change at any specific point in the fixed coordinate system, while the second represents the acceleration which the fluid experiences in sweeping through successive points in the fixed coordinate system. Expressed mathematically, this is

$$\frac{D(\ )}{Dt} = \frac{\partial(\ )}{\partial t} + (\vec{v}\cdot\nabla)(\ )$$

The first term is called the unsteady acceleration, and vanishes if the flow is steady as viewed by a stationary observer. The second term arises because the fluid is experiencing an acceleration as it is convected through the fixed coordinate system; not surprisingly, this term is called the <u>convective acceleration</u>, and in Cartesian coordinates is:

$$(\vec{v}\cdot\nabla)(\ ) = v_x \frac{\partial(\ )}{\partial x} + v_y \frac{\partial(\ )}{\partial y} + v_z \frac{\partial(\ )}{\partial z}$$

Note that the operators $(\partial(\ )/\partial t)$ and $(\vec{v}\cdot\nabla)(\ )$ are <u>scalars</u>, so that the <u>vector</u> momentum equation is

$$\rho \frac{\partial \vec{v}}{\partial t} + \rho(\vec{v}\cdot\nabla)\vec{v} = \sum \text{ forces per unit volume.}$$

The Mechanism of Muscular Contraction

When a muscle contracts, one kind of filament within it slides past another kind. Electron microscopy and other techniques have begun to disclose how the filaments exert a force on each other

by H. E. Huxley

An outstanding characteristic of all animals is their ability to move voluntarily by contracting their muscles. When I summarized our understanding of muscle contraction seven years ago [see "The Contraction of Muscle," by H. E. Huxley; SCIENTIFIC AMERICAN, November, 1958], it had already been determined that during contraction two kinds of filament in voluntary muscle—thick filaments and thin ones—slide past each other so as to produce changes in the length of the muscle. At that time one could offer only a hypothetical description of contraction at a more detailed level; it was assumed that a relative force is somehow exerted between the thick and thin filaments at sites where they are connected by tiny cross-bridges. Now, thanks to advances in electron microscopy and allied techniques, we have been able to substantiate that hypothesis and to learn considerably more about the nature of the interaction of the thick filaments (composed mainly of the protein myosin) and the thin ones (composed of another protein, actin). It appears that at each site where the proteins of the two kinds of filament are in contact one of them (probably myosin) acts as an enzyme to split a phosphate group from adenosine triphosphate (ATP) and thus provide the energy for contraction. The basic problem is to understand how the conversion of chemical into mechanical energy takes place.

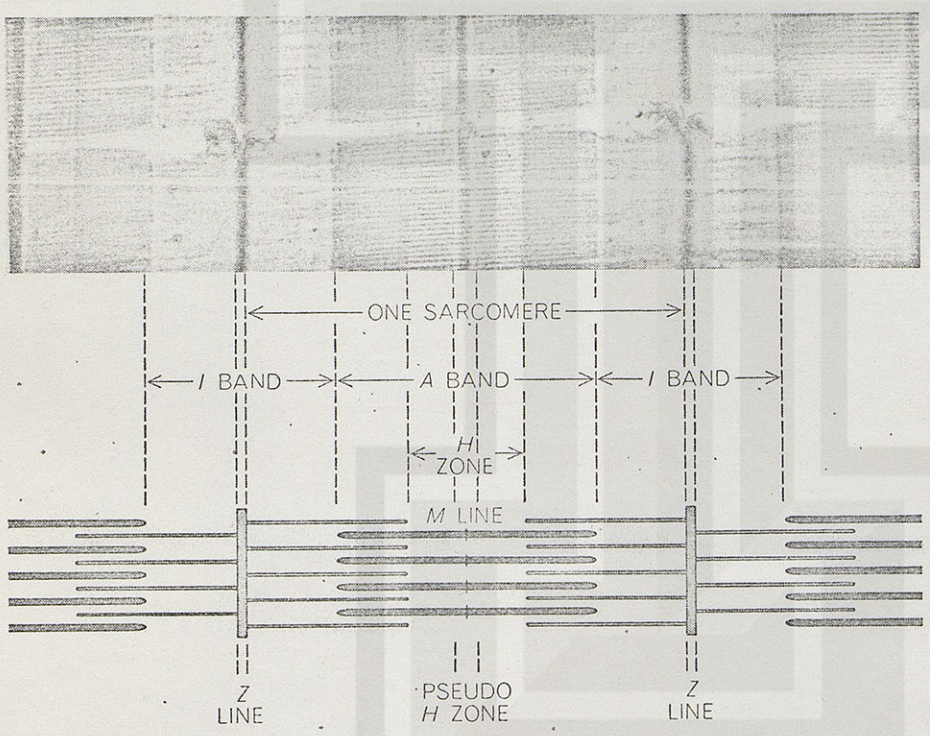

STRIATED MUSCLE from the leg of a frog is shown in longitudinal section in an electron micrograph (*top*) and the overlap of filaments that gives rise to its band pattern is illustrated schematically (*bottom*). Parts of two myofibrils (long parallel strands organized into muscle fiber) are enlarged some 23,000 diameters in the micrograph. The myofibrils are separated by a gap running horizontally across the micrograph. The major features of the sarcomere (a functional unit enclosed by two membranes, the *Z* lines) are labeled. The *I* band is light because it consists only of thin filaments. The *A* band is dense (and thus dark) where it consists of overlapping thick and thin filaments; it is lighter in the *H* zone, where it consists solely of thick filaments. The *M* line is caused by a bulge in the center of each thick filament, and the pseudo *H* zone by a bare region immediately surrounding the bulge. The electron micrograph and others illustrating this article were made by the author.

Let us briefly review what is known about the structure and function of muscle. Under the microscope voluntary muscles—for example those that can move the leg of a frog—appear regularly striated at right angles to their length. The muscles responsible for the slow and regular movements of organs that work involuntarily, such as the gut, appear smooth. For reasons of technical convenience most investigations of muscle have dealt with striated muscle, and so our discussion will refer specifically to muscle of that type. A good deal of what has been learned about striated muscle, however, may apply to smooth muscle as well.

Striated muscle can shorten at speeds equal to several times its length per second; it can generate a tension of some 40 pounds per square inch of its cross section; it can contract or relax in a very small fraction of a second. A muscle consists of individual fibers with a diameter of between 10 and 100 microns (a micron is a thousandth of a millimeter); the fibers run the length of the muscle, or a good part of it. Each fiber is surrounded by an electrically po-

is generally a tenth of a volt negative with respect to the outside. Contraction is signaled by an impulse that travels down a nerve to a motor "end plate" in contact with the fiber. The arrival of the impulse depolarizes the membrane and causes the release throughout the fiber of an activating substance, probably calcium. It is this activation that enables one of the muscle proteins to act as an enzyme and split a phosphate group from ATP. The muscle stays contracted until nerve impulses cease (or until it becomes exhausted), at which point the activating substance withdraws, probably by being bound to the sarcoplasmic reticulum, a network of tiny channels within the fiber.

An individual fiber is made up of a number of parallel elements called myofibrils, each about a micron in diameter. Each myofibril itself consists of parallel actin and myosin filaments that, when they are viewed from the end, are seen to lie a few hundred angstrom units apart in a remarkably regular array. (An angstrom unit is a ten-thousandth of a micron.) The myosin filaments are some 160 angstroms in diameter but often appear somewhat thinner when fixed for electron microscopy. They are about a micron and a half in length. The actin filaments are about a micron in length and 50 to 70 angstroms in diameter. The overlap between the arrays of thick and thin filaments gives rise to the pattern of striations visible in the microscope. The pattern is characterized by a succession of dense bands (called *A* bands) and light bands (*I* bands). In the *A* bands the myosin filaments lie in register in hexagonal array and are responsible for the bands' high density. The actin filaments are attached in register on each side of a narrow, dense structure that traverses the *I* band: the *Z* line. In a relaxed muscle the distance between *Z* lines—one sarcomere—is such that about half of the length of a thin filament and two-thirds of the length of an adjacent thick filament overlap. In the region of overlap in a relaxed fiber the array contains twice as many thin filaments as thick ones. The thin filaments terminate at the edge of the *H* zone, a region of low density in the center of the *A* band. In the center of the *H* zone lies the "pseudo *H* zone," a region of even lower density that maintains its width no matter how the length of the muscle changes. This light zone surrounds a thin, dark strip known as the *M* line, which is now thought to be caused by a slight bulge in the center of each thick filament.

When a longitudinal section of muscle is viewed in the electron microscope, it can be seen that the cross-bridges between a given pair of thick and thin filaments come at fairly regular intervals. The cross-bridges are the only mechanical linkage between the filaments, and they are responsible for the structural and mechanical continuity along the whole length of a muscle. It is the cross-bridges that must generate or sustain the tension developed by a muscle. As the sarcomere changes its length, either actively during contraction or passively (stretching or shortening while at rest), the filaments themselves do not perceptibly change in length but slide past one another; the thin filaments move farther into the *A* bands during shortening and farther out of them during stretching.

Since normal contractions involve changes in the length of the sarcomere of 20 percent or more, the thin filaments in each half of the *A* band must move distances of at least a quarter of a micron while maintaining tension. It seems physically impossible that the cross-bridges could remain attached to the same point on the actin filament throughout this process. We supposed, therefore, that they are attached to one site on the filament for part of the contraction, then detach and reattach themselves at a new site farther along. Moreover, we assumed that at each site

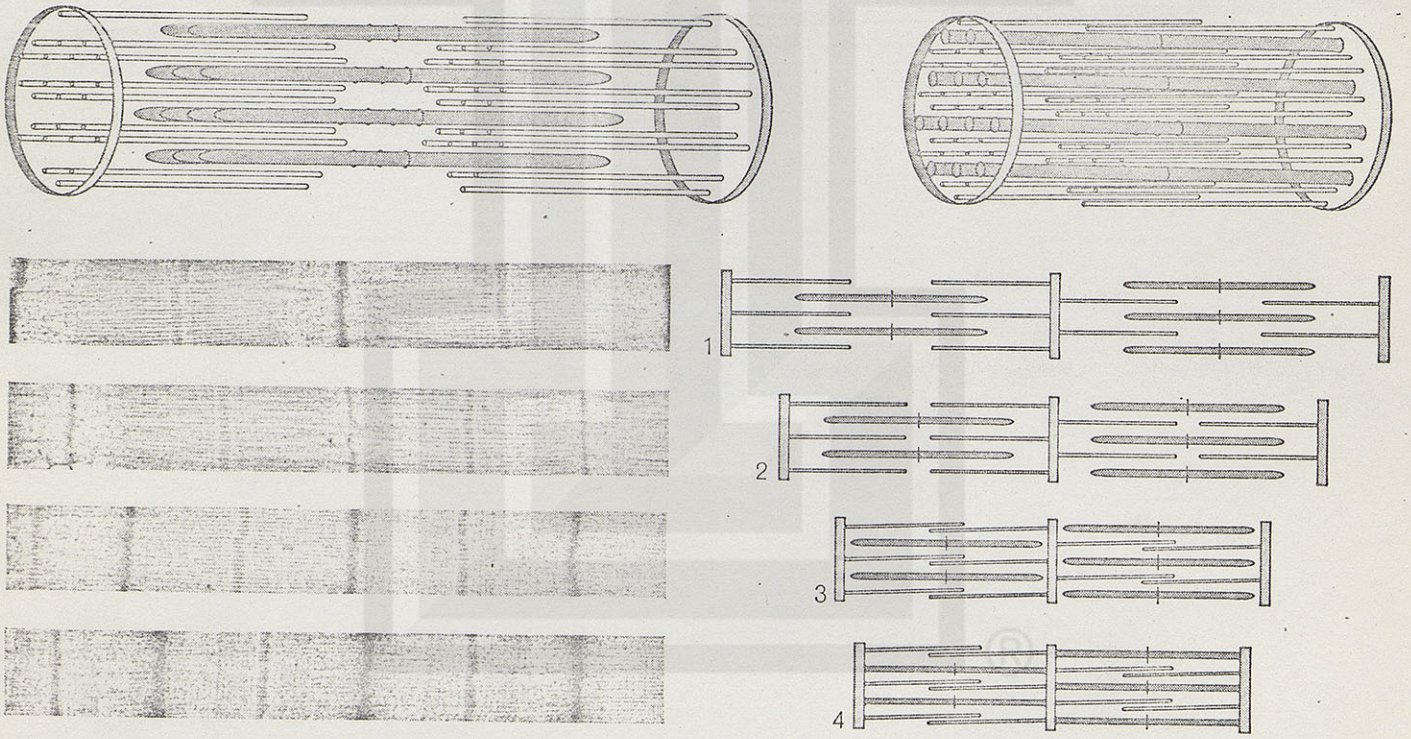

CONTRACTION OF MUSCLE entails change in relative position of the thick and thin filaments that comprise the myofibril (*top left and right*). The effect of contraction on the band pattern of muscle is indicated by four electron micrographs and accompanying schematic illustrations of muscle in longitudinal section, fixed at consecutive stages of contraction. First the *H* zone closes (*1*), then a new dense zone develops in the center of the *A* band (*2, 3 and 4*) as thin filaments from each end of the sarcomere overlap.

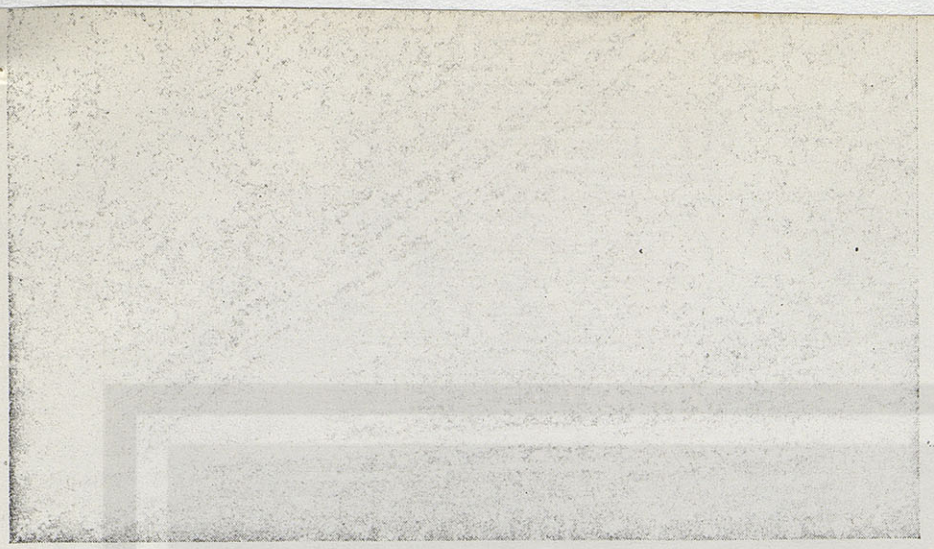

CROSS-BRIDGES between thick and thin filaments are enlarged 180,000 diameters in electron micrograph made by "negative staining." Technique involves surrounding very small objects with a dense salt (*white substance in background*) so that they stand out by contrast.

where cross-bridge and filament interact, one molecule of ATP is split to generate a sliding force between the two kinds of filament (and hence between arrays of filaments).

This general description of the structural changes associated with contraction is the sliding-filament hypothesis put forward a decade ago by Jean Hanson of the Medical Research Council unit at King's College in London and me, and independently by A. F. Huxley and R. Niedergerke of the University of Cambridge. Our hypothesis was partly based on observations of muscle prepared by what is called the thin-sectioning technique. That method involved steeping a chemically fixed (for preservation) and stained (for contrast) piece of muscle in liquid plastic and then cutting the solidified plastic into slices as thin as 100 angstroms. It turned out, however, that the thin-sectioning technique was not adequate to the task of illuminating many details of the hypothesis. In order to ascertain how a force might be developed between thick and thin filaments we needed information about the detailed structure of actin and myosin, and such information was not forthcoming until the arrival of the technique of electron microscopy known as negative staining.

This new method, in which the specimen under examination is embedded in a thin film of some very dense material such as uranyl acetate, has in recent years revealed much about the structure of small spherical viruses and particles of similar size. As adapted in our laboratory at the Medical Research Council unit in Cambridge, the technique involves applying a drop in which particles of muscle are suspended to an electron microscope grid covered by a thin film of carbon. Many particles adhere to this film; the excess is washed away with a few drops of solvent. Before the preparation dries a shallow drop of the negative-staining material—a heavy metal salt in dilute solution—is applied. It is allowed to dry around the particles. The regions of the particles that are not penetrated by the stain show up clearly by negative contrast because they consist of protein and are much less dense than the salt that surrounds them.

The negative-staining method brings to light far more detail than the conventional positive-staining technique (which artificially increases the density of objects with respect to their background). Its disadvantage is that it can only be applied to very thin specimens; thick ones and the associated thick deposit of negative stain would impair the resolution of the electron microscope image. Thus the method is not directly applicable to whole pieces of tissue such as muscle. The muscle must first be broken down into fragments of suitable thickness (such as individual filaments), which is not easily accomplished.

The usual method of breaking down muscle tissue for purposes of investigation is to homogenize it in the Waring blendor; under this treatment it disperses readily into its constituent myofibrils but no further. In fact, the myofibrils probably because the cross-bridges between thick and thin filaments bind the whole structure together in a very robust fashion. Making the assumption that the cross-bridges are the sites where actin and myosin combine, we wondered if we might weaken the structure by suspending the fibrils in certain salt solutions that tend to dissociate the two proteins. We were delighted to find that if muscles, either freshly isolated or preserved in a deep freezer in a solution of water and glycerol, were placed in the appropriate salt solution and then homogenized in the blendor, they indeed broke down into their constituent filaments. Thus they could provide excellent material for examination by the negative-staining technique.

The first specimens we prepared by this method consisted of filaments from the psoas muscle in the back of a rabbit. In the electron micrographs the layer of negative stain was thickest in the region immediately surrounding the filaments; accordingly the filaments have a dense outline [*see illustrations at bottom of opposite page*]. We could at once recognize the thick filaments by their resemblance to the thick filaments in earlier preparations of striated muscle. The diameter of the filaments was the expected 160 angstroms; their length was apparently about 1.5 microns. (Longer structures were never observed but shorter ones, presumably fragments, were.) Small projections, extending sideways from the filaments along most of their length, seemed to correspond to the cross-bridges. Thinner filaments 50 to 70 angstroms in diameter could also be seen, and in places we noticed a large group of such filaments extending for about a micron on each side of a Z line, to which they were still attached [*see illustration at bottom left on opposite page*]. These observations of thick and thin filaments of characteristic size, lying side by side and sometimes still connected by cross-bridges, confirmed the conclusions about the structure of the myofibrils reached earlier by X-ray diffraction techniques and by conventional light microscopy and electron microscopy. We subsequently considered the appearance of the individual filaments more closely.

A regular feature of the thick filaments is a short region, midway along their length, from which the projections we believe to be cross-bridges are absent. This differentiated, projection-free area, some .15 to .2 micron long, can be seen not only in negatively stained

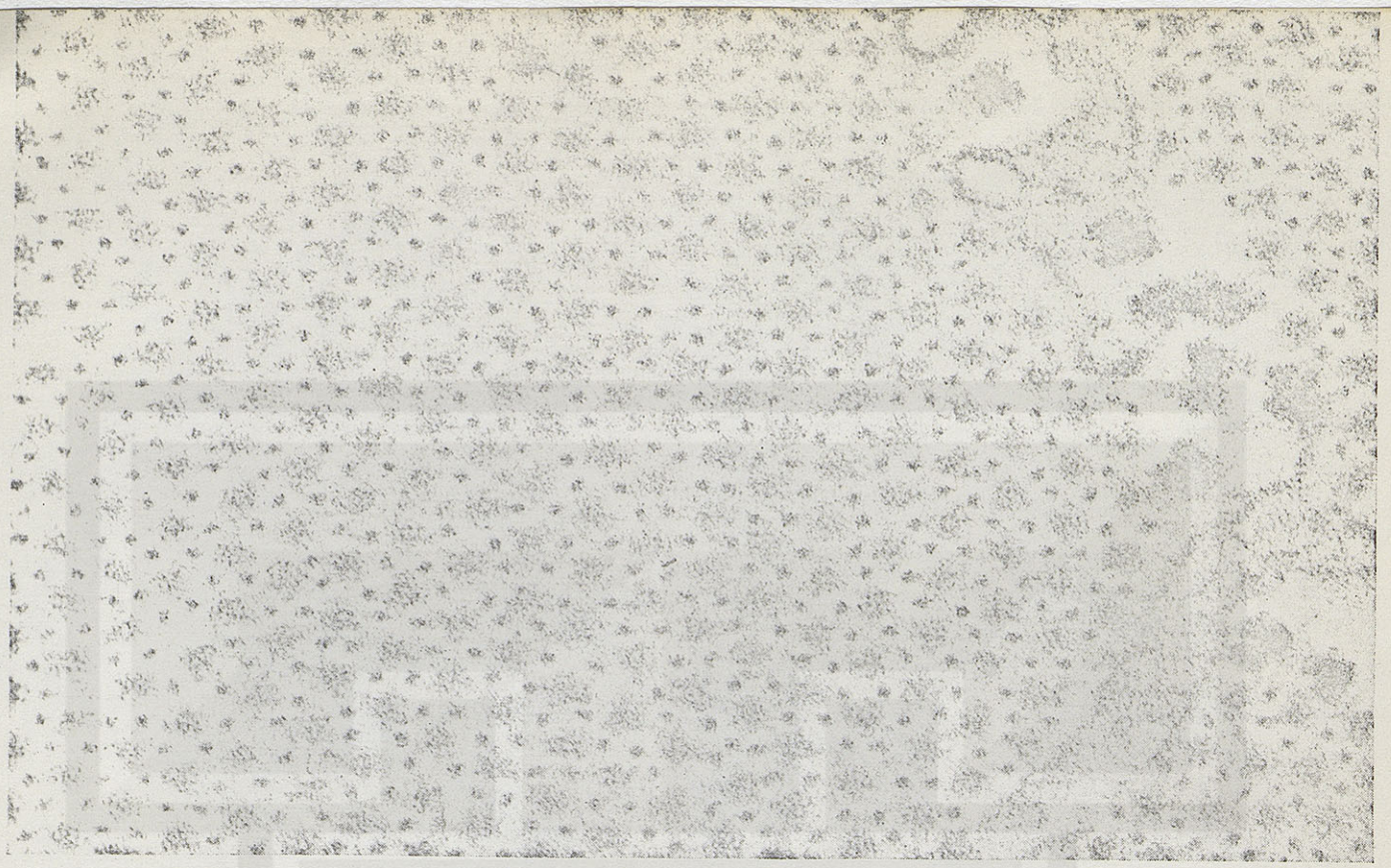

TRANSVERSE SECTION through a frog's leg muscle in its uncontracted state shows how thick and thin filaments are arrayed in a regular hexagonal pattern. Breaks in the pattern at the right side of the micrograph are channels of the sarcoplasmic reticulum. From the end thick and thin filaments look like large and small dots. This electron micrograph enlarges them some 200,000 diameters.

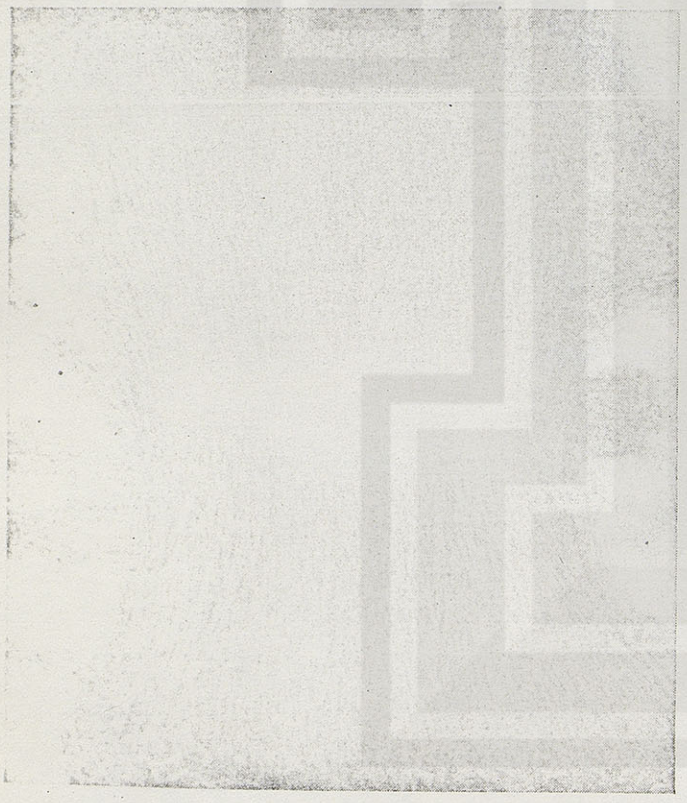

FILAMENTS IN REGISTER at *Z* line (*membrane in center*) are the thin filaments of actin, which alone comprise the *I* segment. This sample was obtained by homogenizing muscle from the back of a rabbit in the Waring blendor; it was prepared for the micrograph by negative staining. Magnification is some 47,000 diameters.

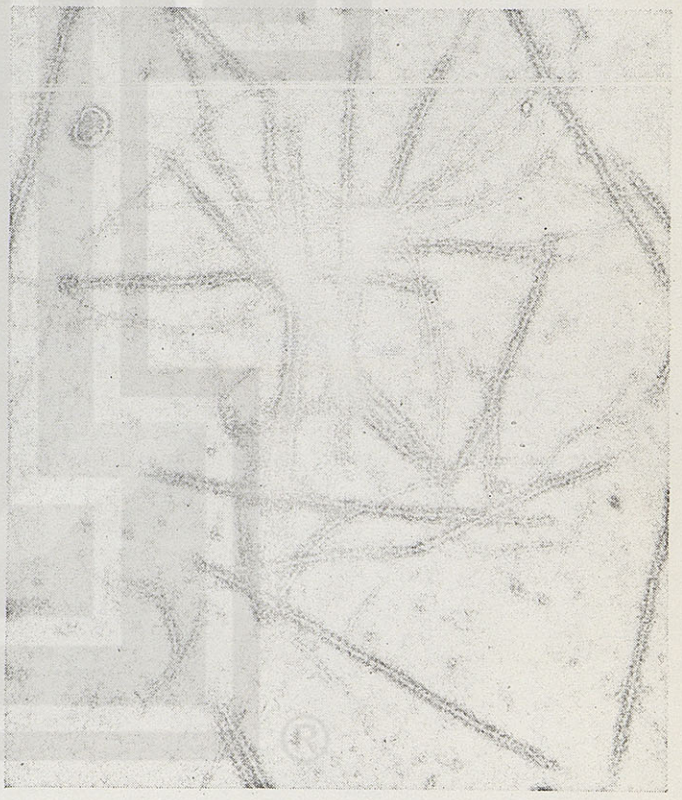

SEPARATED FILAMENTS are from rabbit muscle that has been homogenized in a Waring blendor. The dark, thick strands are filaments of myosin. The very faint thin strands are filaments of actin. Thin filaments are still attached to remnant of *Z* line (*dark patch at top center*). Filaments are enlarged some 35,000 diameters.

material but also in sectioned specimens. It is now apparent that the absence of cross-bridges from this region is responsible for the mysterious pseudo *H* zone. This zone maintains its uniform size at various muscle lengths because it is a structural feature of the filaments themselves and is not created by their pattern of overlap.

At first sight the projection-free middle region of the thick filaments did not seem particularly significant. It was conceivable that the region was composed of some other protein constituent of muscle. The situation was transformed, however, when we found that filaments of virtually the same appearance could be synthesized from purified solutions of myosin, the protein that is the main component of the thick filament.

The myosin molecule is known to be an elongated structure with a length of about 1,500 angstroms and a diameter of 20 to 40 angstroms. It can be split (by the enzyme trypsin) into two well-defined fragments; the fragments were named light meromyosin and heavy meromyosin by Andrew G. Szent-Györgyi of the Institute for Muscle Research in Woods Hole, Mass. The heavy-meromyosin fragment has the ability to split a phosphate group from ATP and the ability to combine with actin. The light-meromyosin fragment possesses neither of these attributes but retains the solubility properties that enable it to form the same kind of structure that intact myosin does. The molecule of heavy meromyosin appears to be more globular than the molecule of light meromyosin. The dimensions of the fragments suggest that before cleavage of the myosin molecule they are arranged in simple end-to-end fashion.

Isolated myosin molecules have been examined under the electron microscope, first by Robert V. Rice of the Mellon Institute in Pittsburgh and subsequently by other workers, by means of the technique known as shadow-casting. This entails treating particles on a film in a vacuum by spraying them at an angle with a vaporized heavy metal.

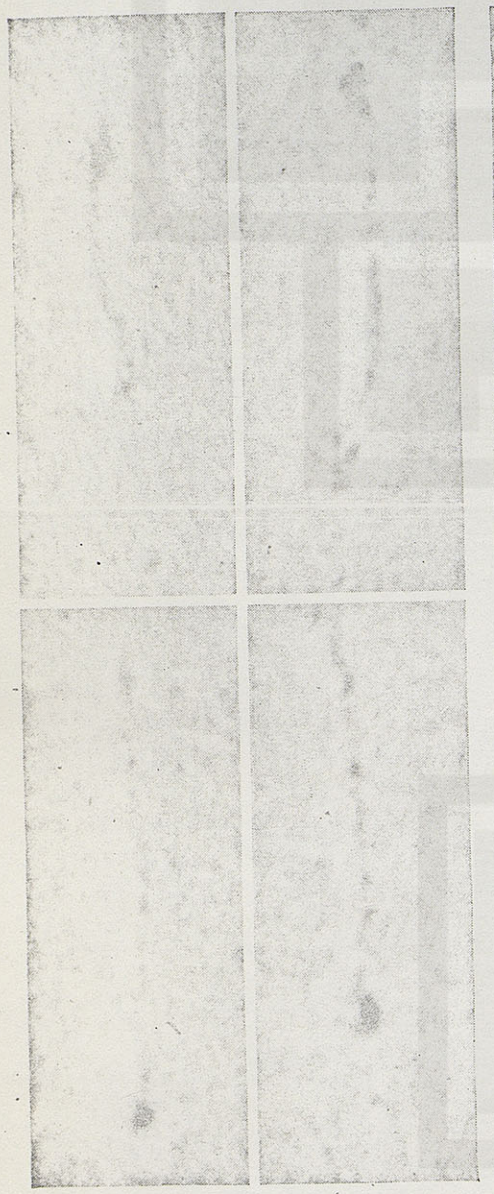

MYOSIN MOLECULES appear in electron micrographs prepared by shadow-casting method. The wide head has enzymatic properties and combines with actin. The straight tail can aggregate with other myosin molecules. Magnification is 300,000 diameters.

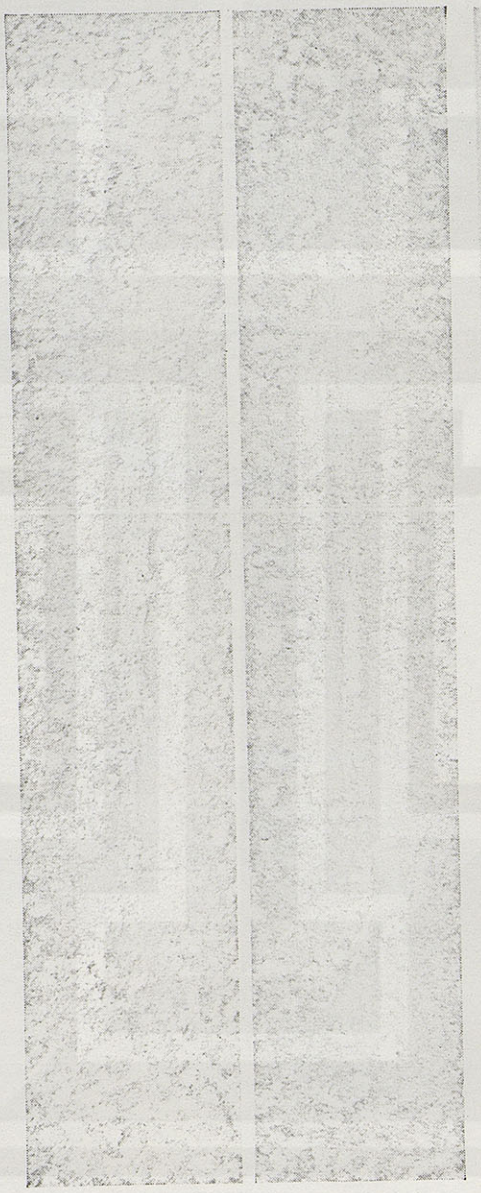

AGGREGATIONS of several molecules from a precipitate of pure myosin were negatively stained and magnified 175,000 diameters to reveal their characteristic appearance: a thick strand with projections near the ends and a bare region in the middle.

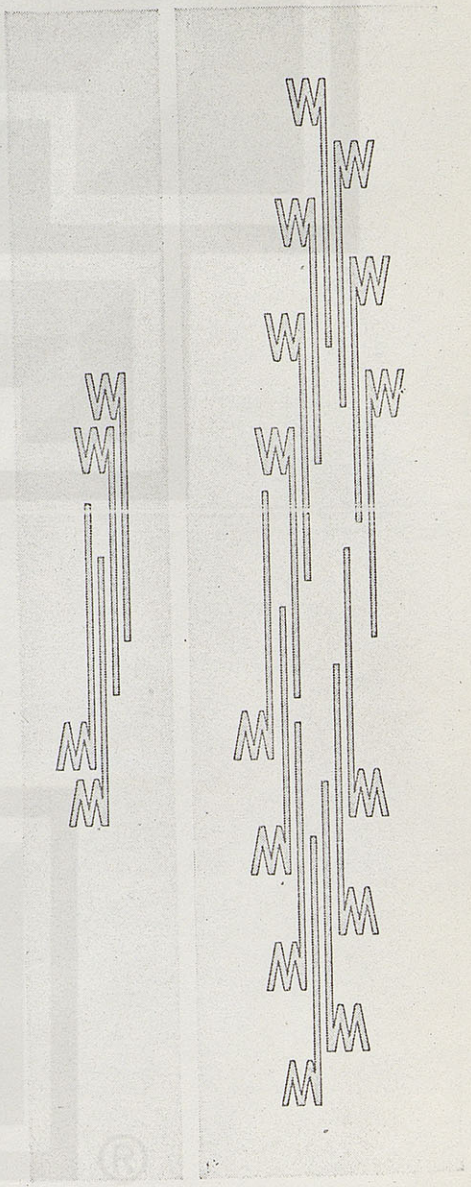

MOLECULAR STRUCTURE of myosin makes it aggregate in the manner shown here. Head of molecule is schematically represented by zigzag line, tail by straight line. Tails join in center; heads extend as projections at ends, oppositely pointed at each end.

metal builds up the particles on the near side and leaves a shadow on the far side, where it is blocked from landing on the underlying film. When myosin molecules are prepared by this method for viewing in the electron microscope, they appear as linear structures with a globular region at one end [*see illustration at left on opposite page*]. Heavy-meromyosin fragments are seen to consist of a large globular head with a short tail. Light-meromyosin fragments appear as simple linear strands. It therefore seems that the intact myosin molecule is asymmetric—a molecule with a head and a tail. The sites (perhaps a single site) responsible for its enzymatic activity and its affinity for actin are located in its globular head, and the sites responsible for its affinity for other myosin molecules are in its tail. The head, which is 40 angstroms in diameter, accounts for about a sixth of the length of the molecule; the tail, 20 angstroms in diameter, accounts for the rest.

It is known that under certain conditions purified myosin in potassium chloride solution will precipitate. When we examined such a precipitate by the negative-staining technique, we were delighted to find that it consisted entirely of filaments. They varied somewhat in length and diameter but generally bore a most remarkable resemblance to the thick filaments prepared directly from muscle. Systematic examination of these synthetic filaments, first of short filaments only two or three times the length of a single myosin molecule and then of longer ones, turned up an even more remarkable feature. The shortest filaments were straight rods some 1,500 to 2,500 angstroms long, with clusters of globular projections at both ends. It occurred to us that we were looking at a small number of myosin molecules arranged in two opposite directions, with their globular heads forming the projections and their linear tails overlapping [*see middle illustration on opposite page*]. Longer filaments had longer clusters of projections, but the projection-free region in the middle of each filament was the same length as the corresponding region in the shorter filaments. The longest synthetic filaments we observed closely imitated the appearance of thick filaments extracted from muscle. It seems clear that myosin filaments grow by the addition of molecules parallel to the molecules that have already aggregated. The molecules are oriented in one of two opposite directions, depending on which end of the filament a given molecule is joining. It is this method of construction that gives rise to the projection-free region in the synthetic filaments and of course to the same feature in the natural filaments.

MYOSIN FILAMENTS were obtained directly from muscle homogenized in a blendor (*four electron micrographs at left*) for comparison with a synthetic filament from precipitate of pure myosin (*micrograph at right*). The thick filaments from muscle and the synthetic filament have the same form, characterized by the bridge-free zone in the center and the projections clustered at each end. The filaments are enlarged some 105,000 diameters.

This study of myosin molecules and the way they aggregate impressed on us two features that explain the role of these molecules in muscle. First, the head of the molecule has the enzymatic and actin-binding properties we have long assumed the cross-bridges must have. Second, because the molecules aggregate with their heads pointed in one direction along half of the filament and in the opposite direction along the other half, they have an inherent directionality. The first observation leads us to conclude that the heads of myosin molecules serve as the cross-bridges connecting the thick and thin filaments in muscle. The second is important because it explains a crucial feature of the sliding-filament hypothesis at the molecular level.

In a sliding-filament system in which a relative force is developed between actin and myosin molecules located in the two types of filament, it is essential that the appropriate directionality of sliding be built into the filaments in some way. In a striated muscle the thin filaments move toward each other in the center of the *A* bands, so that it is required that all the elements of force generated by the cross-bridges in one

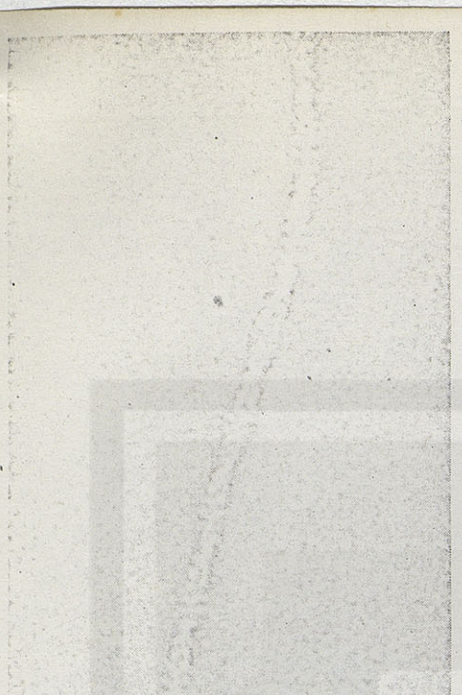

ACTIN FILAMENT has a characteristic structure, visible in micrograph in which filament is enlarged some 420,000 diameters. The filament has the appearance of two coils of globular units wound in a double helix.

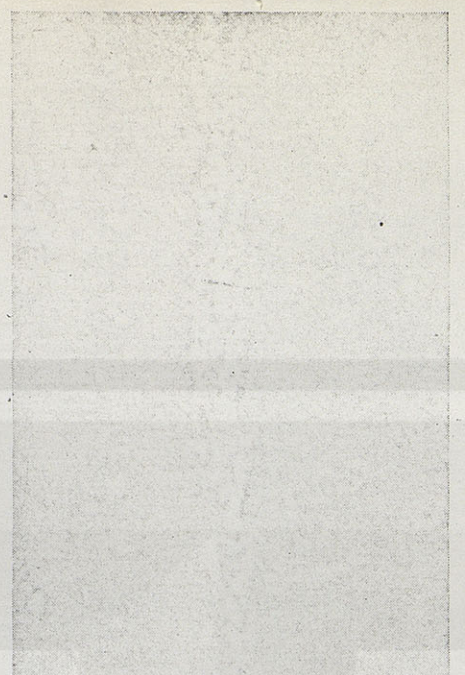

"ARROWHEADS" point in one direction along each filament of actin labeled with heavy meromyosin (extract of the globular halves of myosin molecules), implying that actin has an inherent polarity of its own.

half of the *A* band be oriented in the same direction, and that the direction of the force be reversed in the other half. The direction of the force developed as a result of the interaction of actin and myosin would depend either on the orientation of the myosin molecules, the orientation of the actin molecules or both. Our electron microscope observations suggest strongly that all or part of this directionality is achieved by the fact that the myosin molecules are arranged so that they point in the same direction in half of each thick filament (and hence in each *A* band) and in the opposite direction in the other half [*see illustration at right on page 22*]. Moreover, we have shown that filaments with this essential reversal of polarity at their midpoint will assemble themselves automatically in vitro from purified preparations of myosin; this finding has obvious relevance to problems of how muscle develops its structure.

Let us now turn to the thin filaments. It was first noticed by Jean Hanson and J. Lowy of the Medical Research Council unit in London that the thin filaments from the smooth muscle of clams had a characteristic beaded appearance. They were able to show that the filament had the form of a double helix consisting of two chains of roughly globular subunits, the chains twisted around each other so that viewed from a given direction the crossover points were about 360 angstroms apart [*see illustration at left on this page*].

The thin filaments from striated muscle show an identical structure; it can often be seen even when they are still attached to a *Z* line. Filaments made from actin prepared by standard biochemical techniques again show the same pattern. Thus we can confirm that the thin filaments of striated muscle do contain actin, as we had supposed. We can also deduce that the globular subunits are molecules of actin that aggregate to build up the filament. The structure itself might resemble two strings of beads twisted around each other; its alternating high points and low points suggest a general arrangement for the successive active sites on the filament to which the cross-bridges may attach themselves (assuming that each globular unit has one site). We cannot directly view enough of the internal structure or shape of the subunits to make any deductions about their directionality. To reveal such polarity we have used a natural marker, namely heavy meromyosin, the fragment of myosin that combines with actin.

When actin filaments are treated with a solution of heavy meromyosin and examined in the electron microscope by negative staining, they assume a complex appearance that we do not yet understand in full detail. Nevertheless, one salient feature stands out immediately: the filaments of the resulting compound have a well-defined structural polarity that manifests itself in an obvious arrowhead pattern [*see illustration at right on this page*]. The arrows always point in the same direction over the length of a given filament, even when only dilute solutions of heavy meromyosin have been applied and the arrow pattern is interrupted by long stretches of normal uncombined actin. If the polarity were imposed by some local condition such as the direction along the actin filament at which a series of heavy meromyosin molecules were attached during the formation of the compound filament, one would expect the pattern of arrowheads to lack such consistency. Therefore it would seem that it is the underlying structure of the actin that imposes the pattern. Precisely which feature of the myosin-actin combination gives rise to the arrowhead effect is unclear; it may well be that the pattern reveals the actual orientation of some part of the heavy-meromyosin fragments. A general feature can be deduced, however: all the actin molecules in a filament will combine with heavy meromyosin in precisely the same way [*see top illustration on page 26*]. We can conclude that all

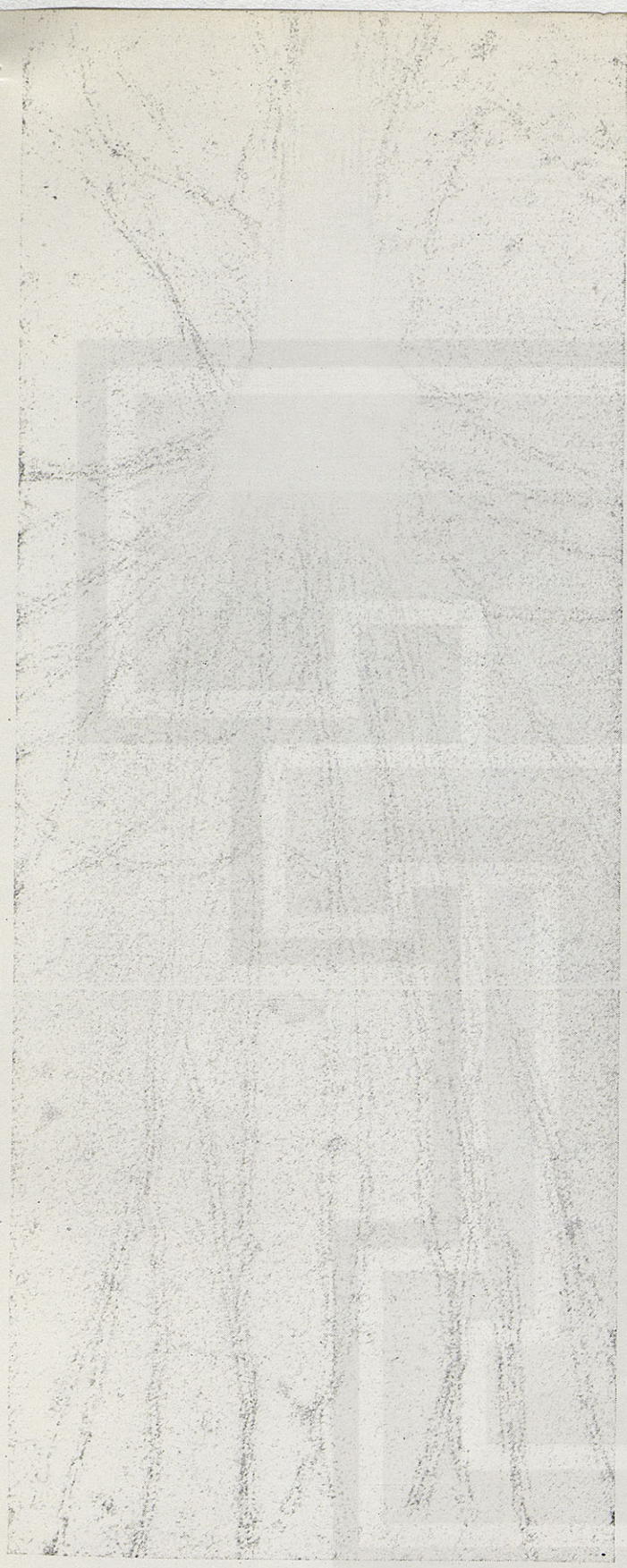

Z LINE, the membrane that forms the end of a sarcomere, appears as dark region from which strands radiate. The strands are thin actin filaments that comprise the *I* band. At times, as in this instance, they remain attached even after muscle has been homogenized. This micrograph and one at right were made by negative staining. They both have magnification of some 165,000 diameters.

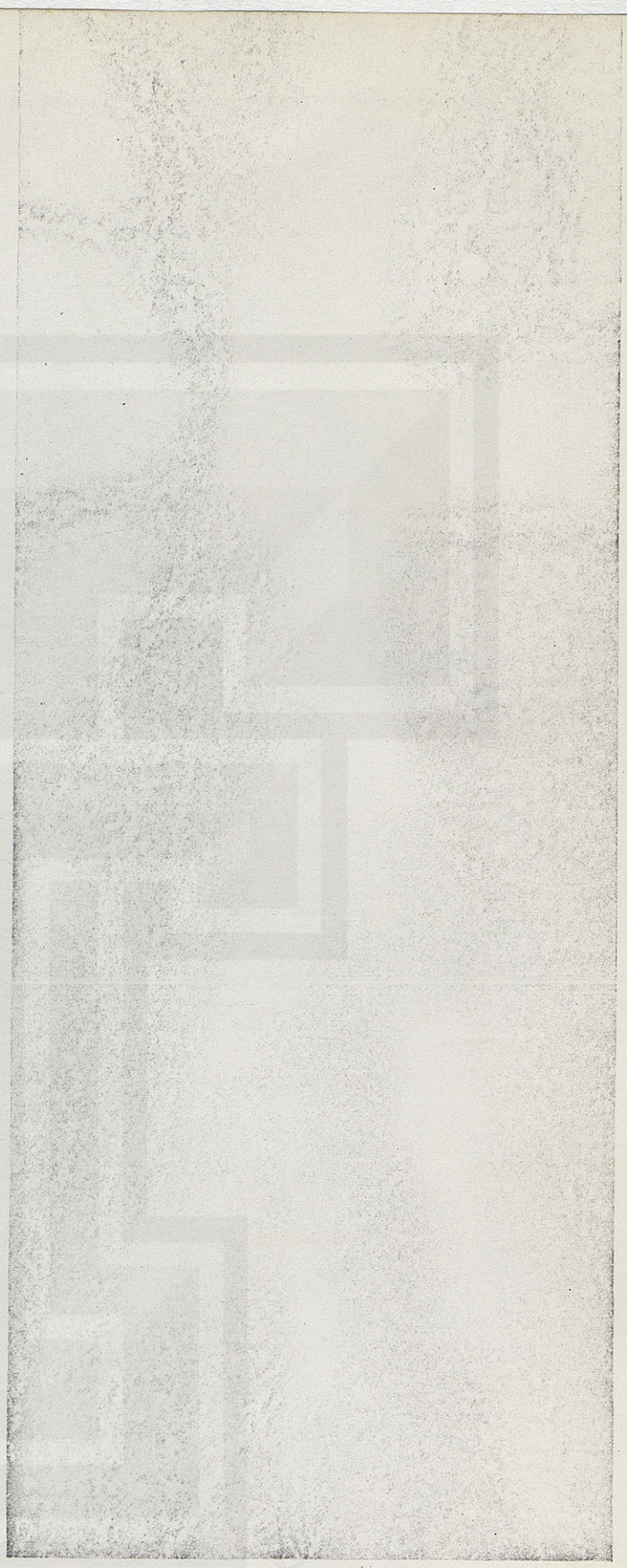

DIRECTIONALITY OF ACTIN is demonstrated when thin filaments attached at the *Z* line are labeled with heavy meromyosin. Arrowheads form, pointing away from the *Z* line on each side. In this micrograph they point up at top of *Z* line, down at bottom. Opposite orientation of the two *I* segments of a sarcomere enables filaments from left and right *I* segments to converge on center.

the actin molecules in a given thin filament are oriented in the same sense and that they can all interact in identical fashion with a given myosin cross-bridge.

We have used the same technique to investigate the way in which the actin filaments are attached at the Z lines. As I have mentioned, preparations of thin filaments from homogenized muscle frequently contain groups of filaments still connected to both sides of a Z line. We find, in examining such assemblies after treatment with heavy meromyosin, that the arrows on all filaments always point away from the Z lines. The filaments forming the *I* substance on one side of a Z line are all similarly oriented; on the opposite side of the Z line the orientation is reversed.

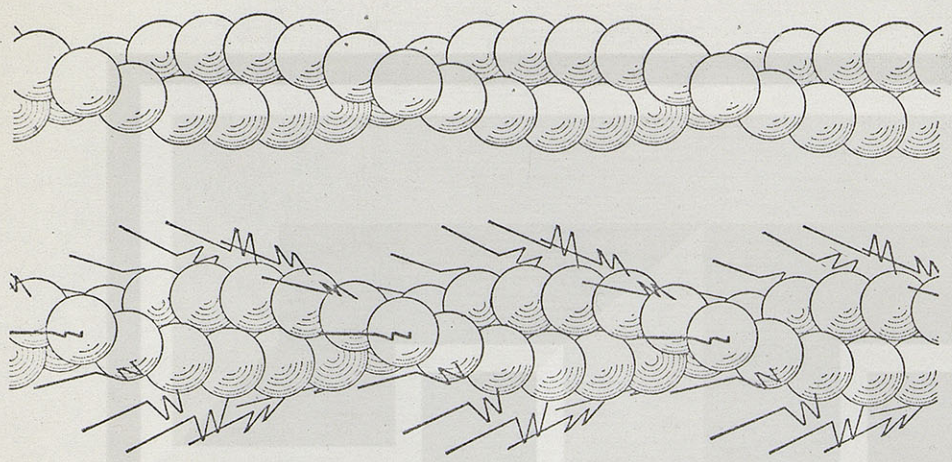

STRUCTURE OF ACTIN is represented by two chains of beads twisted into a double helix (*top*). The way in which actin might combine with heavy-meromyosin fragments to give rise to arrowheads apparent in micrograph at right on page 24 is suggested at bottom.

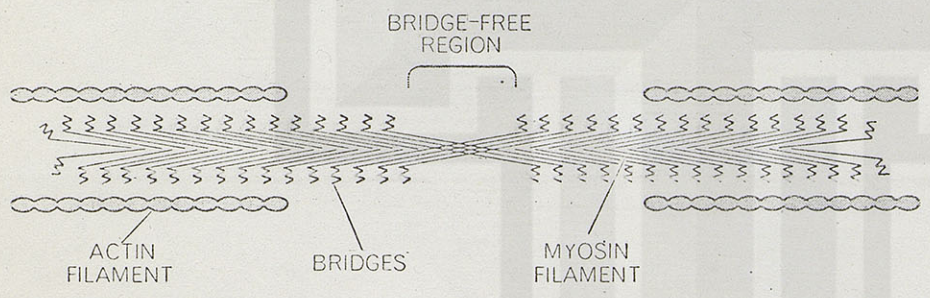

CONTACT OF ACTIN AND MYOSIN in muscle might be made in the manner schematically illustrated here. The thin actin filaments at top and bottom are so shaped that certain sites are closest to thick myosin filament in the middle. The heads of individual myosin molecules (*zigzag lines*) extend as cross-bridges to the actin filament at these close sites.

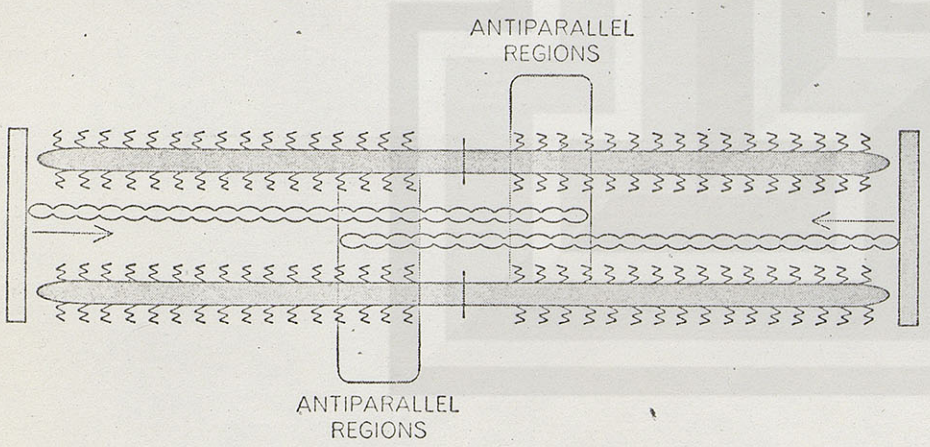

DOUBLE OVERLAP of thin filaments from each side of the sarcomere would result if the sliding-filament hypothesis is essentially correct. It is now assumed that muscle generates maximum tension when thin filaments reach center of *A* band, and that tension falls when thin filaments cross the center and interact with improperly oriented cross-bridges.

This is exactly the arrangement we require in order for the same relative orientation of the actin and myosin molecules to obtain in the two halves of the *A* bands but for the absolute orientation to be reversed. The direction of the forces developed will consequently be reversed and the actin filaments can move in opposite directions, that is, toward each other in the middle of the sarcomere.

We conclude that both the thick and the thin filaments in a striated muscle are assembled and oriented in such a way that if a relative force were developed between a given actin and myosin molecule in either filament, all the elements of force in the whole system would be added together in the appropriate manner to give rise to the organized behavior we have observed. Several years ago we tentatively proposed the analogy of a ratchet to describe the interaction of sliding filaments. Now our understanding of the way in which cross-bridges of myosin seem to hook onto consecutive active sites on the actin filament makes the analogy seem even more appropriate.

Recently we have examined with our improved electron microscope techniques sections of muscle fixed at various stages of contraction. The filament lengths, measured by Sally G. Page of University College London, appear to remain constant and equal to the corresponding lengths in resting muscle (discounting small changes in length from tension during fixation and other preparative steps). The most interesting feature of the contraction sequences we have studied is that at the shorter sarcomere lengths a dense zone appears in the center of the *A* band; the zone progressively increases in width as the muscle shortens. This zone first appears after the *H* zone has closed up completely. We had shown previously that the closing of the *H* zone during shortening is caused by the ends of the thin filaments sliding toward each other in the center of the *A* band. Now when we measured the distance from the Z line to the opposite end of the new dense zone, we found that it was still equal to the length of the thin filaments. We therefore suspected that the new zone might correspond to a region where the thin filaments from each end of the sarcomere overlap [*see illustration on page 19*].

This view was confirmed when we examined cross sections of muscle cut through the region of supposed double

of thick and thin filaments in regular hexagonal array with twice as many thin filaments as thick ones, the pattern was less regular and there were four times as many thin filaments as thick ones [*see illustration at right*]. Apparently we were seeing the thin filaments from both ends of the sarcomere at the same time, and these must have slid past one another during the shortening. This finding confirmed that the simple sliding process describes the behavior of the thin filaments under all conditions. (Objectors had proposed, for instance, that the thin filaments might coil up within the A bands.) The finding also suggested to our group and to A. F. Huxley, who is now at University College London, a possible explanation for the observable decrease in tension generated by striated muscles at sarcomere lengths shorter than resting length. Tension would fall off in the double-overlap region because there is a progressively increasing penetration of the thin filaments from one Z line into the "wrong" end of the A bands. We know that actin molecules in part of a thin filament penetrating the center of the A band would have an abnormal orientation with respect to the adjacent cross-bridges [*see bottom illustration on opposite page*]. Such a region would not be expected to contribute to the development of tension by the muscle, and by interfering mechanically and chemically with the interaction of the correctly oriented actin and myosin molecules it might reduce the tension.

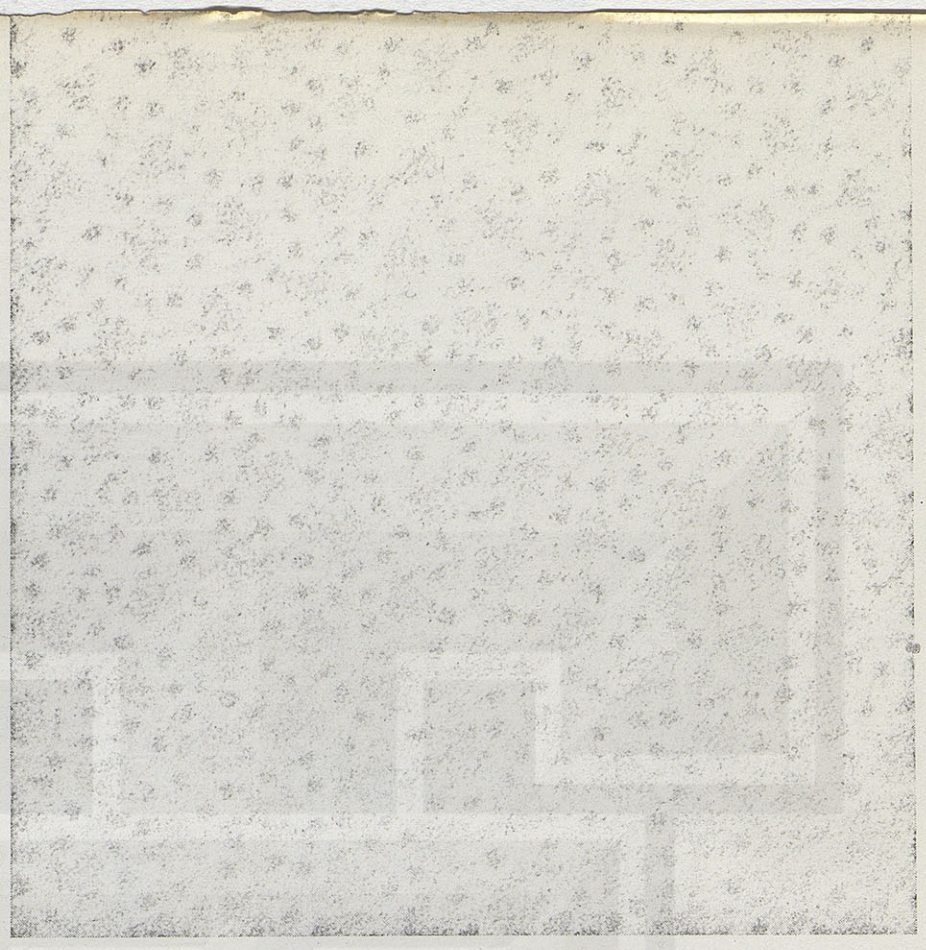

CONTRACTED MUSCLE viewed end on in this electron micrograph has four times as many thin filaments (*small dots*) as thick (*large dots*). The regular array of thick filaments is well preserved; the array of thin filaments is not. Since the ratio of thin to thick filaments in relaxed muscle (*evident in micrograph at top of page 21*) is two to one, it appears that actin filaments from each end of the sarcomere overlap during contraction. This transverse section, made by cutting through the center of an *A* band of a muscle from the leg of a frog (the method used in making section at top of page 21), is enlarged 250,000 diameters.

Can we extend our investigations to consider changes in the arrangement or configuration of the actin and myosin molecules in muscles that are actually contracting? This goal has indeed been attained, thanks to the sophistication of a technique long used in the study of muscle: X-ray diffraction. Untreated muscle reflects X rays in a regular pattern. We can compare the way in which contracted and relaxed muscles reflect X rays and thus determine if activation and the development of tension are associated with appreciable changes in the length of the repeating units of pattern formed by the arrangement of actin and myosin molecules within the filaments (and hence with possible changes in filament length). Two groups of workers—W. Brown, K. C. Holmes and I in Cambridge, and G. F. Elliott, Lowy and B. M. Millman at the Medical Research Council Biophysics Research Unit at King's College in London—have independently conducted such studies, and both groups report that no such changes in length occur during contraction.

Another exciting finding, reported by our group, is that the relative intensity of some of the X-ray reflections associated with myosin filaments changes greatly during contraction. (Subsequently the London group reported observations consistent with our findings.) These effects have still to be analyzed in detail, but they indicate a substantial movement of the cross-bridges during contractile activity. Very recently members of our group and a group of investigators under J. W. S. Pringle at the University of Oxford have demonstrated a movement of the cross-bridges associated with the contraction of insect flight muscle. These latest findings open up new possibilities. Now that we know that measurable changes in the X-ray reflections do in fact occur during contraction, we have a method of distinguishing steps in the process by which energy for contraction is obtained.

A contracting muscle offers a uniquely favorable system for studying the outstanding problems of protein structure and function. In muscle we have now clearly identified the interacting protein molecules, the high concentration in which they are present and their regularity of arrangement. The major unsolved question about contractility is a general question of biochemistry: how do proteins act as catalysts for biochemical reactions, and what happens to them in the process? It is interesting in this regard to recall that ATP itself was first identified as the source of energy in the contraction of muscle and subsequently as the universal carrier of chemical energy in the living cell. We expect that the study of the precise basis of contractility will also lead to broadly applicable results.

Myocardial Ultrastructure in the Normal and Failing Heart

EDMUND H. SONNENBLICK *Harvard Medical School*

The first article in a new series on cardiac failure focuses upon the sarcomere as the basic contractile unit within the myocardium. The phenomena observable under the electron microscope are related to the functioning of the heart as a pump. And it is shown that derangements at the sarcomere level can be related to compensatory mechanisms that ultimately lead to heart failure.

The performance of the heart as a pump is primarily dependent on the contractile activity of the myocardium; the contraction of the myocardium in turn reflects the summated and integrated working of its individual contractile elements — the sarcomeres. This premise is the rationale for examining the ultrastructure of the heart in relation to the continuum of cardiac function: a continuum that extends from normal performance to advanced failure.

Starting from this premise, this article will discuss, in order, the structural and functional components of the sarcomere, the mechanisms through which the phenomena observable in the sarcomere become relevant to myocardial behavior, and the relationships between derangements at the ultrastructural level and the development of cardiac failure.

The ultrastructure consists simply of those morphologic features that are adequately observable only with the resolution and magnification afforded by the electron microscope. The myocardium is composed of numerous interconnecting, branching fibers or cells, each 5μ to 10μ in diameter; these fibers are, of course, visible under the light microscope. Longitudinally the fibers contain irregular rodlike structures or fibrils. The electron microscope shows that the fibrils run the length of the fiber and are composed along their length of regular, repeating structures — the sarcomeres, the ultimate unit of contraction in heart as well as skeletal muscle. The sarcomeres give the fibrils their striped or striated appearance. Sarcomeres in turn are composed of two sets of rodlike filaments, thicker ones composed of aggregates of *myosin* molecules, thinner ones of aggregates of *actin*. Interactions between actin and myosin at specific sites along the filaments produce contraction of the myocardium. Other regulatory proteins have been discovered within the sarcomere, located along the thin actin filament. These include the complex of *tropomysin* and *troponin* whose role will be discussed later.

Functionally the myocardial "machinery" has three components. There is a system to activate and relax the cell, i.e., turn it on and off; an "apparatus" for generating force and shortening; and a system for providing the energy for operating the cell. The activation-relaxation system is related to a series of membranes covering and within the cell. Covering the fibers externally is the *sarcolemma*, the membrane that carries the electrical activity across the surface of the cell.

Cardiac fibers (or cells) branch widely and at their ends the sarcolemma is modified to join cells together into a "functional syncitium." This modified cell surface membrane is called an *intercalated disk* and serves the purposes of holding cells together while providing pathways of low electrical resistance between cells. In addition the sarcolemma invaginates the fibers to carry electrical activity deep into the cells, forming the transverse tubular or *T system*. I would emphasize that both the intercalated disk and the T system are essentially specialized extensions of the sarcolemma.

Inside the cell, surrounding the contractile machinery, is the sarcoplasmic reticulum, another system of fine membranous tubules that abut both the sarcolemma and the T system at specialized terminals or *junctions*. When electrical activity is transmitted within the cell it triggers the release of an activator, presumably calcium, from the sarcoplasmic reticulum and activates, i.e., "turns on" the cell. Conversely, when the sarcoplasmic reticulum reabsorbs the calcium, the contractile machinery of the cell is inactivated.

The aerobic energy system of the myocardial cell is contained within mitochondria, which lie between the myofibrils and, as in other cells, utilize food substances and

Dr. Sonnenblick is assistant professor, Harvard Medical School, and director of cardiovascular research, Peter Bent Brigham Hospital, Boston.

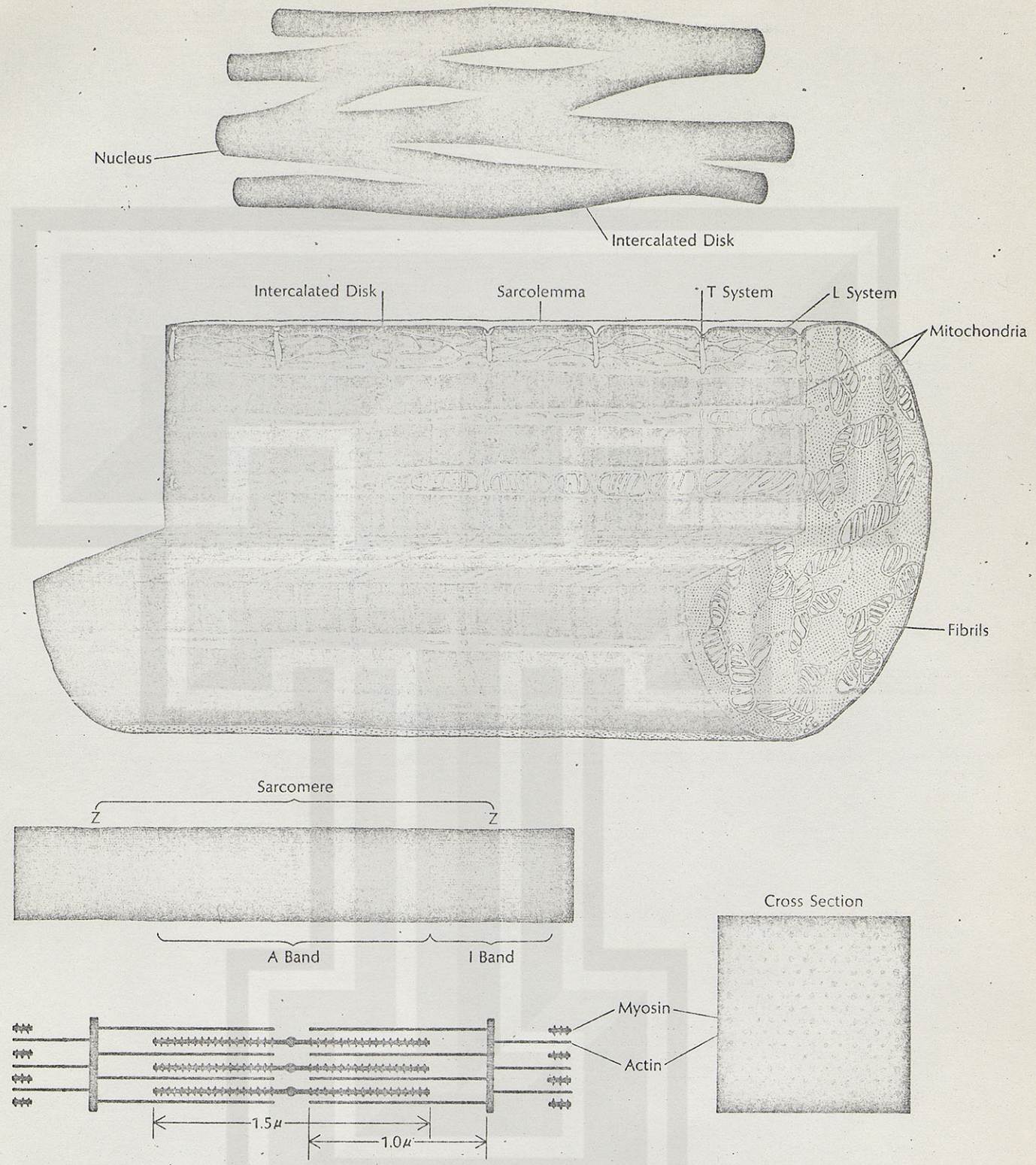

Myocardial structure, as seen under the light and electron microscopes, is schematized. Top drawing shows section of myocardium as it would appear under light microscope, with interconnecting fibers or cells attached end-to-end and delimited by modified cell membranes called intercalated disks. Ultrastructural schematization (center drawing) illustrates the division of the fiber longitudinally into rodlike fibrils, in turn composed of sarcomeres, the basic contractile units. Within the sarcomeres, thick filaments of myosin, confined to the central dark A band, alternate with thin filaments of actin which extend from the Z lines (delimiting the sarcomere) through the I band and into the A band where they overlap the myosin filaments. These landmarks are seen in detail drawings (bottom). On activation a repetitive interaction between the sites shown along these filaments displaces the filaments inward so that the sarcomere and hence the whole muscle shortens, with maximum overlap at 2.2μ. Also depicted are the membranous systems – the T- and L-systems that carry electrical activity into the cells and release calcium to activate the contractile machinery. Like the intercalated disks, these are specialized extensions of the superficial sarcolemma. Also noteworthy is the rich mitochondrial content, typical of "red" muscle, which is highly dependent on aerobic metabolism.

oxygen to produce adenosine triphosphate (ATP), the direct energy source for myocardial contraction.

This brings us to the contractile machinery, the sarcomere, which constitutes about 50% of the myocardial fiber. This is an appreciably lower percentage of contractile protein than is found in skeletal muscle, where upward of 80% to 90% of total mass is contractile fibers. This difference reflects mainly the greater amount of mitochondria in heart muscle.

With the electron microscope the the outstanding topographic feature of the sarcomere is its banded appearance – alternating bands of dark and light repeating from sarcomere to sarcomere. Alternations in the repetitive banding of the sarcomere reflect the relative disposition and overlap of the two sets of protein filaments that interact to produce the force of contraction.

At both ends of the sarcomere, there are thin dark lines which are called Z lines. The Z lines provide insertion points for the thin actin filaments from the two abutting sarcomeres. While the detailed structure of the Z line is still not fully clarified and varies somewhat from muscle to muscle, it has the general appearance of a straw mat into which the thin actin filaments are interwoven. Although as a matter of convenience we have been referring to the thin filaments as being composed of actin, troponin is now known to be associated with the actin and plays a major role in regulating interaction of actin and myosin.

At the sarcomere center is a broader dark area, the A band, composed of the thicker myosin filaments. Between the dark Z lines and the dark A band are two lighter zones, the I bands. Thin filaments extend inward from the Z lines through the I bands and end near the center of the A band. The thick filaments run the length of the A band. In the lateral portions of the A band there is thus an overlap of thick and thin – myosin and actin – filaments. In longer sarcomeres a relatively lighter zone appears at the central portions of the A band, which is termed the H zone. The H zone represents that portion of the A band where only thick filaments are present.

In recent years, we have been able to gain an increasingly clear understanding of the nature of the force generators along the myofilaments, although definition is still far from complete. At the center of the A band, the thick filaments are connected by fixed bridges that hold these filaments in relative position and create a darkened area of cross banding along the M line. Along the thick filaments, projections extend out at intervals of 400 Angstroms. At rest, troponin, which is located periodically along the actin filament, inhibits the interaction of these projections with the actin filament. When calcium is available to interact with troponin, this inhibition ceases and bridges are formed between myosin and actin. An enzyme in the myosin portion of the bridge for splitting ATP (an ATPase) is activated; the bridge then generates force and the filaments are displaced relative to one another. This leads to a breaking of the bridge that can then be reformed further on along the filament. In this repetitive fashion and through the summation of such bridge formations, contraction is generated.

Because the degree of overlap of filaments determines to a considerable extent the degree of interaction, the normal lengths of the filaments are extremely important in visualizing the process. The thick myosin filaments are approximately 1.5μ in length; the thin actin filaments measure about 1.0μ. Present evidence strongly suggests that the absolute length of the filaments remains constant during the resting period and in the course of contraction. When the cell is activated however, a repetitive interaction occurs between sites along these filaments. This interaction effectively pulls the thin filaments inward toward the center of the A band, shortening the sarcomere and hence the muscle. This process gives us the "sliding model" for muscle contraction, clearly established for skeletal muscle and now well documented for the myocardium as well. Since the number of active sites on the myosin filament that will come into contact with the actin depends on the degree of overlap, the overlap primarily determines the force generated between the two sets of filaments. One other fact is revelant. There is a section of the thick filament at its center, about 0.2μ, that is devoid of reactive sites.

A number of variables have now been defined, which, taken together, can be seen to relate most significantly to the functioning of the myocardium and to the possible effects of dilatation on such function. The thick myosin filaments are 1.5μ in length and occupy the central portion in the sarcomere. The thin actin filaments extend inward from the Z lines 1.0μ in each direction. Taking into account the inactive region in the middle of the myosin filament, the optimal length of the sarcomere — the length at which maximum overlap and force of contraction occur — is seen to be 2.2μ.

To understand the import of this sarcomere length it is necessary to turn to some of the kinetics governing the functioning of the heart as a pump. A necessary starting point is Starling's law of the heart, which in its simplest form states that the heart will pump out the blood that is returned to it from the venous system on a beat-to-beat basis, and that both the initial size of the heart (prior to contraction) and the volume of blood ejected will be determined primarily by the volume of blood returned to it from the circulation. This may be exemplified with figures derived from experiments with the intact dog's heart. If the initial or end-diastolic ventricular volume is 40 cc, the output with contraction or stroke volume will be about 20 cc, or 50% of initial volume. If the dog then lies down, causing a sudden increase in venous return that raises the end-diastolic volume to 50 cc, the following contraction will eject 25 cc of blood. The ejection fraction, i.e., stroke volume/end-diastolic volume, remains essentially constant and the stroke volume is determined primarily by the end-diastolic volume. Of course these relations are also affected by the load against which the heart is pumping, i.e., the pressure, and by the "contractility" of the ventricle at that moment, but the example serves for general illustration. As venous return and ventricular end-diastolic volume rise, so does ventricular end-diastolic pressure. The phenomenon takes place in both the right and left sides of the heart, providing a balance between the two sides of the circulation. An inevitable result otherwise would be the displacement of excessive systemic

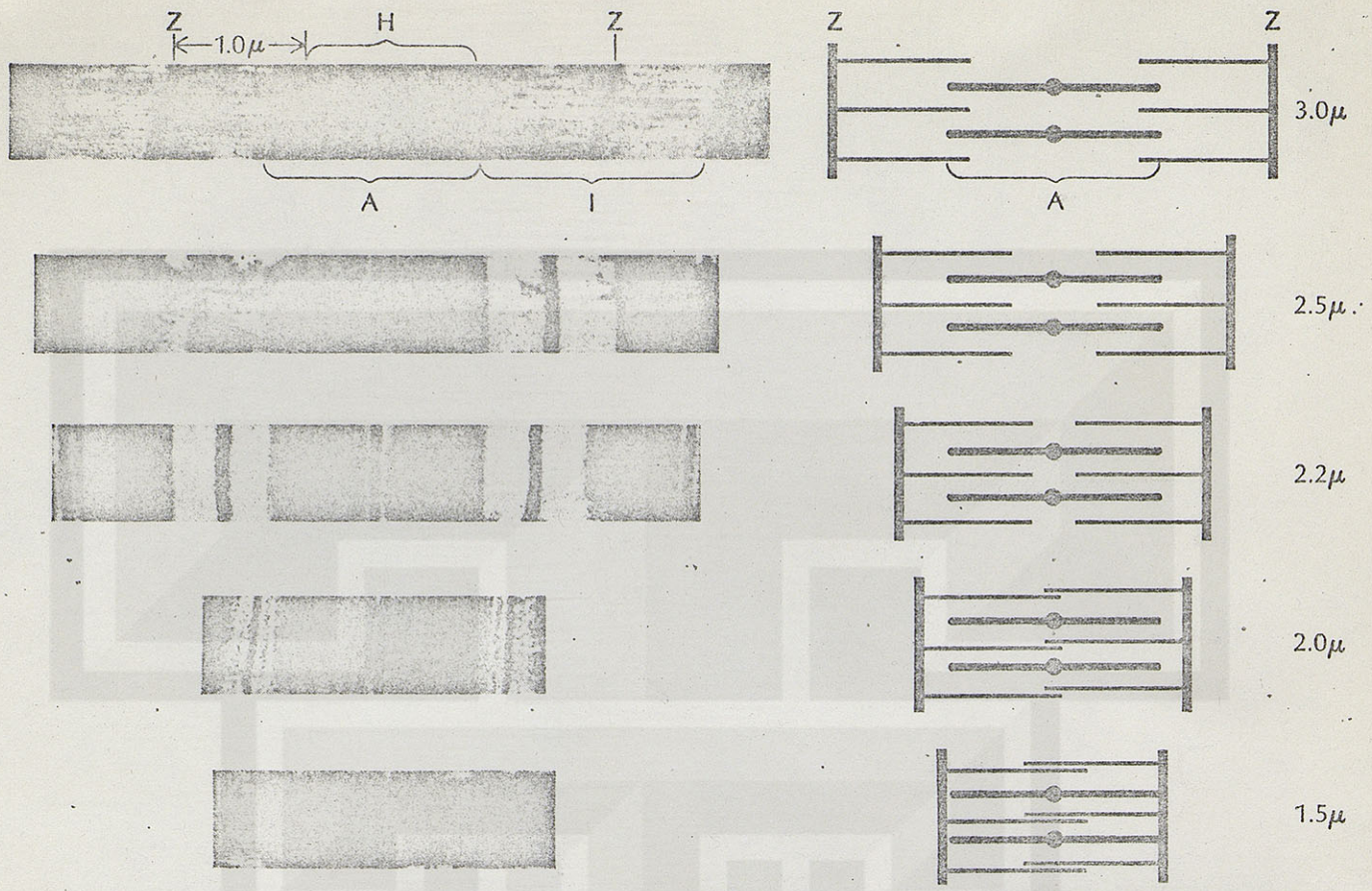

The way in which altering sarcomere length changes band pattern is shown in actual frog sartorius muscle sarcomeres (left) and in correlated diagrams. The middle sarcomere is at L_{max} (2.2μ), at which length maximum contractile force is produced.

blood into the pulmonary vascular bed, with attendant pulmonary edema, or the total depletion of the pulmonary vascular volume.

Starling's law of the heart is based on the fact that the heart is a muscle and, more precisely, a muscle that pumps. Certain characteristics hold for all muscle. First, initial muscle length and contractile force are related. There is a muscle length at which the developed tension produced by a muscle will be maximum (L_{max}). If muscle length is either increased or decreased from this point, a decrease in developed tension occurs, i.e., a decrease in the force that the muscle can produce. By plotting length of muscle against the tension it produces, one can derive the length-active tension curve for that muscle. There is also a length-passive tension relationship for muscle – that is, the tension generated when the muscle is not being actively stimulated but simply being stretched. In heart muscle, the length-passive tension curve is reflected in the relation between the end-diastolic volume and end-diastolic pressure. Because the heart normally doesn't operate at L_{max} but at a point somewhat lower, i.e., on the ascending limb of the length-active tension curve, an increase in the passive tension will strengthen the muscle and cause more blood to be ejected. This accounts for the change in the output of the heart that corresponds to increased initial size, and, of course, also provides the heart with reserve capacity and with the ability to compensate in certain situations.

Other mechanical and geometric considerations must be kept in mind. First is the LaPlace relation which states that the tension in the wall of a sphere is directly related to the pressure in and the radius of the cavity, and inversely related to the thickness of the wall. Thus, if the end-diastolic volume is increased, the tension generated in the wall in systole must be higher to develop the same pressure to open the aortic valve and eject blood. As tension in the wall is increased, a decrease in the extent of shortening during systole will occur. Because of geometric considerations, the same stroke volume could still be ejected with decreased shortening as the ventricle enlarges. However, if an increased stroke volume is to be produced in direct relation to the increased end-diastolic volume, the extent of shortening must be restored despite the increased tension load. Accordingly, one must move up the length-active tension curve of the muscle fibers in the wall of the heart.

Why does the Starling curve reach a peak? Here again one can relate physiologic events to the length-tension curve for muscle. As one ascends the length-tension curve, a point (L_{max}) is reached where further stretching of the muscle will not result in increased developed tension. Therefore, the sarcomeres and the whole muscle will not shorten as much and the heart will not expel more blood despite increased volume. In an attempt to compensate for the deficit in output the heart will continue to get larger. The individual with the failing

heart may no longer operate on the ascending limb of the length-active tension curve but rather near its apex. Here he has lost the ability to generate increased tension by augmenting end-diastolic volume. This is one explanation for the discomfort such a patient feels when he assumes the recumbent position. A large volume of blood moves into his chest, increasing the size of his heart. The filling pressure on the left ventricle rises since this chamber cannot expel the increased blood volume delivered to it. Pulmonary capillary pressure rises and the patient develops shortness of breath and signs of pulmonary congestion.

Let us relate these dynamics now to the ultrastructure of the heart, and specifically to the sarcomere length. It will be recalled that force development in muscle is directly dependent on the amount of overlap between the thick and thin filaments of contractile protein, with optimal overlap achieved at a sarcomere length of 2.2μ.

If one takes isolated muscle (skeletal or cardiac) and fixes it at various lengths one can correlate overall muscle length with sarcomere length. Such correlations have established that over a wide range, the length of the sarcomere is directly related to the length of the muscle. The same muscle can also be studied in terms of its length-active tension curve. This is done in the muscle bath by stretching the muscle; one can then stimulate the muscle while maintaining the same stretch and determine how much tension it will produce at the particular length when activated. Having determined the relationship between tension and length in the muscle, the muscle is fixed in the bath, and sarcomere length determined; the latter can now be directly related to the length-tension curve.

Not only is there a definite and direct relationship between sarcomere and muscle length, but there are certain predictable lengths for the sarcomere that can be correlated with the length-tension curve. At the top of the length-tension curve, sarcomere length is about 2.2μ. This, of course, is the length already noted at which optimal overlap exists between the myosin and actin filaments that are responsible for cardiac contraction. Clearly the length-tension curve is much more than a mathematical construction. It represents an extremely significant reflection of physiologic events within the myocardium.

As muscle and sarcomere lengths are reduced, there is a linear fall in the muscle tension. And as muscle length and sarcomere length are increased beyond the apex of the curve, the actively developed tension again falls.

At first glance, this would seem to be the reverse of what might be expected with increased muscle length. In fact, resting (passive) tension continues to rise when the apex of the length-active tension curve is passed. But active tension – the tension that the muscle can develop over and above the resting tension – starts to decline when muscle length is increased to a point that increases sarcomere length beyond approximately 2.2μ. In skeletal muscle preparations, as one continues to stretch the muscle, sarcomeres continue to elongate. An H zone appears and continues to widen while active tension falls progressively to zero – at a sarcomere length of 3.5μ. This figure is interesting; it can also be arrived at by adding the lengths of the thin filaments (1.0μ each) and of the thick filament (1.5μ). In short, if all overlap between thick and thin filaments is removed, no tension can develop. In effect, the thick and thin filaments appear to have slid past each other, removing all sites for interaction and therefore all force generation.

In cardiac muscle, the changes in the elongated sarcomere are not as straightforward. If myocardium is overstretched, it becomes extremely stiff, possibly because of the surface membranes, connective tissue elements, or some factor inherent in the sarcomere. If heart muscle is stretched 20% or 30% beyond L_{max}, the active tension it can generate will fall from about 10 gm/cm^2 to perhaps 2 or 3 gm/cm^2, while the resting tension will rise to 70 or 80 gm/cm^2. This precipitous rise in resting tension limits how far one can stretch myocardium.

"Slippage" is another factor that must be reckoned with in evaluating the relationship between the ultrastructural features of the myocardium and its performance. As the heart muscle is overstretched – let us suppose the cardiac *muscle* length is increased to 30% above L_{max} – the linear relationship between muscle and sarcomere length no longer holds entirely. In this situation the *sarcomere* may be only 10% longer than at L_{max}. H zones appear in such elongated sarcomeres in overstretched heart muscle

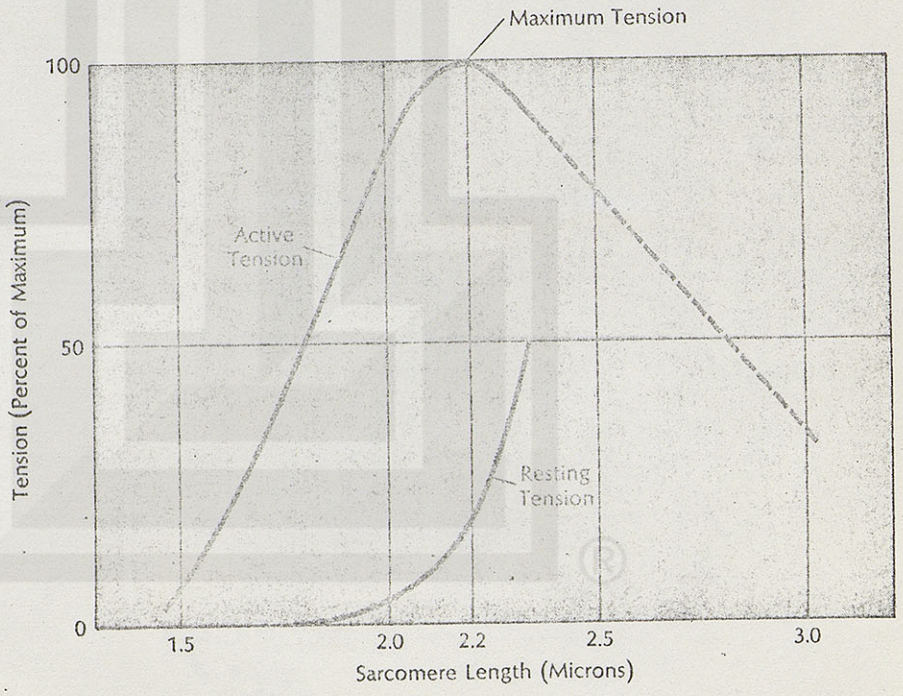

The relationship between tension development and sarcomere length in cardiac (cat papillary) muscle is shown by two curves, the lower one representing resting tension and the upper one representing active tension. It is interesting to note that cardiac muscle has considerable resting tension in contrast to most skeletal muscle.